Electro-optical effects in liquid crystals

L. M. Blinov

Scientific Research Institute of Organic Intermediates and Dyes
Usp. Fiz. Nauk **114**, 67–96 (September 1974)

This review gives information on the electric and optical properties of liquid crystals (LC), and discusses in detail various electro-optical effects in nematic, cholesteric, and smectic LC. Dielectric deformations of LC in electric fields, electrodynamic instabilities, the electromechanical effect, etc., are treated. Special attention is paid to explaining the physical reasons for the change in the optical properties of thin LC films when acted on by an electric potential. The practical applications of LC in electro-optical devices are briefly reviewed.

CONTENTS

1. INTRODUCTION. GENERAL INFORMATION ON LIQUID CRYSTALS

Liquid crystals are liquids in which a definite ordered arrangement of molecules exists, with consequent anisotropy of mechanical, electric, magnetic, and optical properties. The liquid-crystalline state arises under certain conditions in organic substances having sharply anisometric molecules, i.e., molecules that have a clearly marked elongation in one of the directions, or are flat. A good example of such a substance is p-methoxybenzylidene-p′-n-butylaniline (abbreviated MBBA),

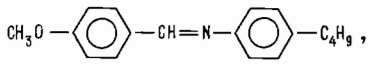

which shows a liquid-crystalline phase of the simplest type (nematic) over a certain temperature range (21–47° C).

Nematic liquid crystals (NLC) are characterized by long-range orientational order and complete translational freedom of the centers of gravity of the individual molecules in space, as well as freedom of rotation of the molecules about their long (and sometimes also short) axes (see Fig. 1a, where the dashes denote the molecules of a NLC). A model of a nematic phase might be a pencil box that one gently shakes to imitate thermal motion: if one doesn't shake it very hard, the pencils shift around, but remain parallel to one another. Upon strong shaking, the box will contain complete disorder. The thermotropic[1)] NLC behave similarly: they are usually solid crystals at low temperatures; a phase transition to a nematic state (melting point) occurs with rising temperature; and a second phase transition occurs at a still higher temperature to an isotropic-liquid state (clearing point).

Cholesteric liquid crystals (CLC) are a variety of nematic substances. Here also, orientational but not translational order exists. However, the CLC are formed by substances having optically active molecules (which rotate the plane of polarized light). The asymmetry of these molecules leads to a twisted structure in the liquid crystal. In Fig. 1b the solid dashes show the arrangement of molecules in the layer of the CLC closest to the observer, while the molecules in a deeper layer are rotated by a small angle φ with respect to the molecules of the first layer (this is shown by the dotted dashes). The angle φ increases for successive layers, and the specimen as a whole forms a helix with an axis perpendicular to the axes of the molecules and the plane of the drawing). Examples of substances that form CLC are the esters of cholesterol or the optically active isomers of compounds of the type

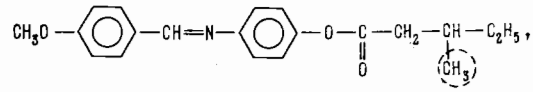

where the optical activity is caused by the asymmetric arrangement of the CH_3 groups in the long tail of the molecule (the temperature range of the cholesteric phase of this substance is 35–76° C).

A second important class of liquid-crystalline substances is the smectic liquid crystals (SLC), which are characterized by one-dimensional translational order as well as orientational order (Fig. 1c). A SLC is closest in structure to solid crystals, and in substances that form both a nematic and a smectic phase, it is not fortuitous that the sequence of phase changes upon lowering the temperature is:

isotropic liquid → NLC → SLC → solid crystal.

An example is the following substance, with a range of existence of the metastable smectic phase of 61–35° C:

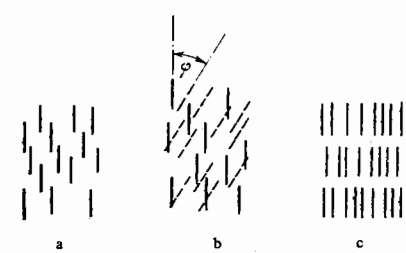

FIG. 1. Structure of liquid crystals of the nematic (a), cholesteric (b), and smectic (c) types.

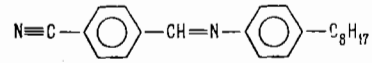

It is pertinent to ask what are the concrete substances that tend to form a liquid-crystalline state. People have tried repeatedly to devise a molecular-statistical theory of liquid crystals, i.e., infer their thermodynamic properties from the electronic structural features of the molecules. It is now generally thought that dispersion (van der Waals) attractive forces between the molecules and steric repulsive forces play defining roles in producing the liquid-crystalline state. The most important molecular characteristic that governs the tendency of a concrete substance to form a liquid-crystalline state is anisotropy of electronic polarizability. In this sense, long, rodlike molecules with benzene molecules lying in a row are most favored. A positive factor is the existence of a conjugated chain (alternation of single and double chemical bonds) along the entire skeleton of the molecule, because the conjugation enhances the longitudinal component of the molecular polarizability. Apparently, existence of a permanent dipole moment in molecules is not correlated with ability of the substance to form liquid crystals, although it often determines their electric and electrooptical properties. The shape of the end groups of the molecules (the steric factor) is highly essential. For example, as a rule, the butyl group ($n\text{-}C_4H_9$-) facilitates getting liquid crystals at very low temperatures: elongation of the end groups reduces the anisotropy of the polarizability, owing to "twisting" of the molecule, while shorter groups bind the molecules too rigidly, and thus raise the phase-transition temperature.

More detailed information on the structure and properties of liquid crystals can be found in the review [1] and in the book [2] by Chistyakov. The chemical and physicochemical aspects of liquid crystals are discussed in [3,4], while the technology of liquid crystals and their application in electrooptical devices are discussed in [5]. Kapustin's monograph [6] has described in rather great detail the results of the early studies on the electrooptics of liquid crystals. The aim of this review is to discuss from a unified standpoint the physical mechanisms of the electrooptical phenomena, and based on this, to discuss the results of some new publications on this topic.

2. ANISOTROPY OF ELECTRIC AND OPTICAL PROPERTIES OF LIQUID CRYSTALS

Quantitatively, the degree of order of a liquid crystal is defined by the orientational order parameter S introduced by Zwetkoff [7]:

$$S=\frac{1}{2}(3\overline{\cos^2\Theta}-1); \qquad (1)$$

Here Θ is the angle between the axis of an individual molecule of the liquid crystal and the preferred direction of the entire ensemble, while the averaging is performed both over the ensemble and over time. The preferred direction coincides with the optic axis of a liquid single crystal, and it must be fixed by an external factor (the wall of the cuvette, a field, or a flux). In line with the sense of the definition, the degrees of order are S = 1 for solid crystals and S = 0 for an isotropic liquid phase. In a liquid crystal, $0 < S < 1$, and S fully determines the anisotropy of the electric and optical properties. In particular, the anisotropy of the diamagnetic susceptibility, as well as the electronic part of the dielectric constant of a liquid nematic crystal, are determined in terms of the anisotropy of the same substances in the solid phase (e.g., in p-azoxyanisole):

$$\Delta\chi_{NLC} = \chi_{\parallel} - \chi_{\perp} = S\Delta\chi_{solid},$$
$$\Delta\alpha_{NLC} = \alpha_{\parallel} - \alpha_{\perp} = S\Delta\alpha_{solid}. \qquad (2)$$

More complicated relationships hold for the anisotropy of the refractive index ($\Delta n = n_{\parallel} - n_{\perp}$), which is connected to $\Delta\alpha$ by the Lorenz-Lorentz relation, for that of the total dielectric constant, which includes an orientational component ($\Delta\epsilon = \epsilon_{\parallel} - \epsilon_{\perp}$), and for the anisotropy of the electric conductivity ($\Delta\sigma = \sigma_{\parallel} - \sigma_{\perp}$). However, the general rule of monotonic decline is maintained for all of these quantities: Δn, $\Delta\epsilon$, $\Delta\sigma \to 0$ as $S \to 0$. The viscosity and elasticity of liquid crystals are also anisotropic.

Figure 2 shows typical temperature dependences of the degree of order, of the refractive index measured with the direction of polarization of the light parallel ($n_{\parallel}$) and perpendicular ($n_{\perp}$) to the optic axis of a NLC, and of the electric conductivity for an electric field parallel ($\sigma_{\parallel}$) and perpendicular ($\sigma_{\perp}$) to the optic axis, and the analogously-defined components of the dielectric constant ($\epsilon_{\parallel}$ and $\epsilon_{\perp}$). We should note that $\Delta n > 0$ in all known NLC and SLC, in line with the anisotropy of the electronic polarizability of the molecules. Yet the sign of $\Delta\sigma$ differs for NLC and SLC in agreement with the anisotropy of the viscosity, which determines the anisotropy of mobility of the charge carriers. In a NLC (with rare exceptions [46]), $\Delta\sigma > 0$, because the charge carriers migrate more readily in the direction of the long axes of the molecules. Conversely, in a SLC the mobility of the charge carriers is higher in a direction along the smectic layers, i.e., perpendicular to the axes of the molecules, and hence $\Delta\sigma < 0$.

The dielectric anisotropy of liquid crystals can be either positive (dotted curves in Fig. 2c) or negative (solid curves in Fig. 2c). This depends on the relationship between the anisotropy of polarizability of the molecule and the value of the permanent dipole moment, and also on the angle ψ between the dipole moment and the long molecular axis. A positive $\Delta\epsilon$ is characteristic of molecules having a longitudinal dipole moment ($\psi \to 0$); $\Delta\epsilon < 0$ happens when the angle ψ is large, e.g., $\psi \to 90°$. Figure 3 gives the frequency-dependences of $\epsilon_{\parallel}$ and $\epsilon_{\perp}$ for two typical NLC that have $\Delta\epsilon\ (\omega \to 0) > 0$ (Fig. 3a) and $\Delta\epsilon\ (\omega \to 0) < 0$ (Fig. 3b). We see that the sign of $\Delta\epsilon$ can change in the frequency range of Debye dipole relaxation, and as will be shown below, this is just what determines the electrooptical behavior of liquid crystals.

Now it is easy to understand wherein lies the specifics of electrooptical effects in liquid crystals. Any process

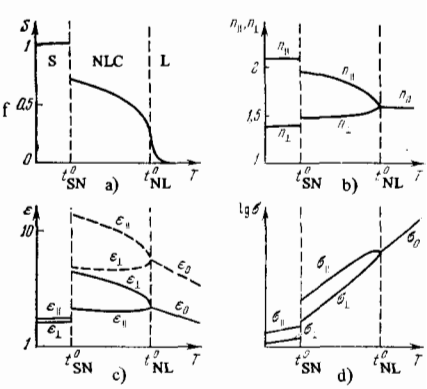

FIG. 2. Characteristic temperature-dependence of the degree of order (a), refractive index (b), dielectric constant (c), and electric conductivity (d) of NLC. t^0_{SN} and t^0_{NL} are the temperatures of the phase transitions solid → NLC, and NLC → isotropic liquid, respectively.

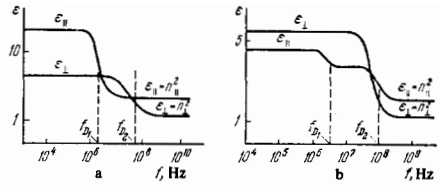

FIG. 3. Typical frequency-dependences of the dielectric constant of NLC for $\Delta\epsilon > 0$ (a) and $\Delta\epsilon < 0$ (b). The Debye relaxation frequencies differ for rotation of the molecules about the short (f_{D_1}) and long (f_{D_2}) axes.

of switching of their optical properties by an external electric field is divided into three stages:

a) Owing to the anisotropy of the dielectric constant and of the electrical conductivity, a liquid monocrystal (analogously to a solid crystal) will experience a torque that tends to reduce the energy of the anisotropic object in the electric field. For example, when $\sigma = 0$, the crystal tends to rotate in such a way that the direction of the maximum dielectric constant coincides with the direction of the field.

b) Owing to the relatively small viscosity and internal friction of the liquid, the torque actually reorients the liquid monocrystal in a relatively short time (this would not happen with solid crystals because of the frictional forces).

c) Owing to the large anisotropy of the optical properties (the refractive indices and the absorption coefficient), any change in the structure of the specimen is easily established optically, in full analogy with the properties of solid crystals.

Thus, all of the unusual character of the electrooptics of liquid crystals arises from the coexistence of properties characteristic of solid crystals and of liquids, while the variety of structures (NLC, CLC, and SLC) and of physical parameters ($\Delta\epsilon$, $\Delta\sigma$, Δn, anisotropy of viscosity and elasticity, etc.) and of boundary conditions gives rise to a large number of different electrooptical effects.

3. ELECTROOPTICAL EFFECTS IN NEMATIC LIQUID CRYSTALS

The first studies of the effect of an electric field on light absorption and birefringence of NLC were carried out as early as 1918.[8] In this and in subsequent studies of the twenties and thirties,[9] fundamental attention was paid to the mechanism of orientation of NLC by an electric field and the interpretation of this phenomenon on the basis of the theory of "dipole swarms", which has now lost currency. At that time, optically transparent electrodes had not yet been invented, and this greatly hampered electrooptical experimentation with thin layers of NLC. Freedericksz and Zwetkoff[10-12] carried out very reliable experiments by using polarized light and wire net electrodes. Unfortunately, these studies have been little cited in the articles of the sixties and the seventies, although they anticipated many of the ideas that the modern theory and applications of the electrooptical effects are based on. Thus, in[10] they describe the intense movement ("boiling") of a NLC of p-azoxyanisole in low-frequency fields, which is accompanied by strong light scattering, i.e., in essence a "dynamic scattering effect," which was discovered anew in 1968.[71,72] They also showed in[10] that there was a critical frequency of the field above which movement vanished, and that the threshold voltage is independent of the thickness of the layer of liquid crystal. They noted[10,11] the role of space charge and the orientational action of the flow of the liquid in the mechanism of anomalous orientation of a NLC having negative dielectric anisotropy. And finally, an important criterion for electrohydrodynamic instability of a NLC was first formulated in[12], namely that $\Delta\epsilon < 0$, as is shown experimentally by varying the size and sign of $\Delta\epsilon$ by adding methoxycinnamic acid to p-azoxyanisole.

We shall first discuss below two cases of very simple electrooptical effects in NLC (deformation by a field and the electromechanical effect), and then we shall go on to electrohydrodynamic instabilities and dynamic scattering.

a) Deformation by an electric field. The basis of practically all experimental studies of the electrooptics of liquid crystals (nematic, cholesteric, and smectic) is the thin-film cell (thickness d = 5—100 μm) with two transparent electrodes 1 on glass substrates 2 (Fig. 4a). There is a capillary gap between the electrodes that is fixed by the dielectric gaskets 3. One can apply to the electrodes a d.c., sinusoidal, or pulsed voltage 4. The light passes through the sandwich along the z axis perpendicular to the electrodes. Polarized light, and in a number of cases monochromatic, is used to study deformations of NLC by an electric field. Depending on the sign of the dielectric anisotropy and the initial orientation of the molecules of the NLC, one can observe three varieties of deformations:

1) Let $\Delta\epsilon > 0$, while the initial orientation of the molecules (Fig. 4b) is characterized by an arrangement of the optic axis of the NLC (or the "director" L) parallel to the electrodes along the axis Ox (L ∥ Ox). Then the layer of NLC shows birefringence with the definite value Δn. The electric field acts against the elastic force of interaction of the molecules with the wall to give rise to a "transverse bending" deformation of the NLC (an S-deformation, from the English word splay), which is characterized by the elastic modulus K_{11}.[13] In a strong enough field, the director is reoriented along the Oz axis, and the birefringence vanishes ($\Delta n \to 0$). This effect is given different names: controlled birefringence, the orientational effect,[15] normal deformation,[14] controlled path difference, etc. We find it most suitable to call it the S-effect because of its brevity and because the letter S recalls the shape of the deformation.

2) Let $\Delta\epsilon < 0$, while L ∥ Oz in the initial state (perpendicular orientation; Fig. 4c). In this case the birefringence vanishes, but reappears when the field is applied to the layer of liquid crystal. The field tends to set the director perpendicular to the Oz axis (because $\Delta\epsilon < 0$). In some cases (e.g., with the additional application of a magnetic field or special physicochemical treatment of the electrode), it tends to set it along a definite direction x or y. The consequent "longitudinal bending" deformation is characterized by the elastic modulus

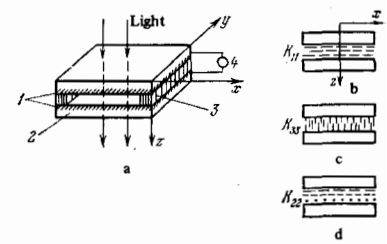

FIG. 4. Electrooptical cell (a) and different cases of orientation of a NLC: S-orientation (b), B-orientation (c), and T-orientation (d).

K_{33}.[13] (B-deformation, from the English word bend). The corresponding electrooptical effect, besides the terms already cited above, is also called the DAP-effect[29] (deformation of a vertical aligned phase). Hereinafter we shall call it the B-effect, in line with the arguments given in Sec. 1.

3) A third type of deformation arises when $\Delta\epsilon > 0$ in the initial orientation shown in Fig. 4d. Here $\mathbf{L} \parallel Ox$ at one of the electrodes, but $\mathbf{L} \parallel Oy$ at the other. Consequently the NLC acquires an optically-active structure twisted by one-fourth turn. This structure rotates the plane of polarization of the transmitted light beam by exactly 90°.[83] The electric field tends to set the director along the axis Oz ($\Delta\epsilon > 0$), giving rise to a deformation in which the rotational elastic modulus K_{22} plays an important role.[2)][13] (T-deformation, from the English word twist). The optical activity vanishes after the NLC has become reoriented; the corresponding electrooptical effect is called the twist effect (the T-effect in our classification).

We can also imagine a reverse twist effect for the case of the orientation $\mathbf{L} \parallel Oz$, $\Delta\epsilon < 0$, with special preparation of the glass windows for a preferential orientation of the NLC in the electric field along x at one electrode and along y at the other. However, such an effect has not been described in the literature.

1) Theory. The theory of deformation of a NLC by an electric field and the birefringence calculation[14-16] have been constructed by analogy with the treatment of the deformation of a NLC by a magnetic field.[17] The difference consists in the fact that we cannot consider the anisotropy of the dielectric constant to be small in comparison with the mean dielectric constant,[16] as happens with the magnetic analog. This is the system of calculation: first one writes the expression for the free energy of the liquid crystal F as a function of the orientation $\mathbf{L}$ of the director and the electric field $\mathscr{E}$ (in the CGSE system):

$$F = \frac{1}{2}\int \left\{ K_{11}(\operatorname{div}\mathbf{L})^2 + K_{22}(\mathbf{L}\operatorname{rot}\mathbf{L})^2 + K_{33}[\mathbf{L}\times\operatorname{rot}\mathbf{L}]^2 - \frac{\Delta\varepsilon}{4\pi}\mathscr{E}(\mathbf{L})^2 \right\} dv, \tag{3}$$

Here $\Delta\epsilon = \epsilon_{\parallel} - \epsilon_{\perp}$, while we have discussed the meaning of the elastic constants K_{ii} above.

Then we solve the Euler's equation corresponding to the functional F, with account taken of the boundary conditions (the different cases of initial orientation of the NLC). We get thereby the steady-state solution that relates the orientation angle Θ of the director to the coordinate along the z axis (see Fig. 4) and to the external field. Here it turns out that the process of reorientation of the liquid crystal shows threshold behavior, and the voltage U_0 across the cell at which reorientation begins is determined by the expression

$$U_0 = \pi\sqrt{\frac{4\pi K_i}{\Delta\varepsilon}}, \tag{4}$$

Here $K_i = K_{11}$ for an initial S-orientation (see Fig. 4b), $K_i = K_{33}$ for a B-orientation (Fig. 4c), and $K_i = K_{11} + \frac{1}{4}(K_{33} - 2K_{22})$[18] for a T-orientation (Fig. 4d).

One can understand the meaning of Eq. (4) from simple physical notions: reorientation begins at the voltage $U_0 = \mathscr{E}_0 d$ (d is the thickness of the cell) at which the density of electrostatic energy $\Delta\epsilon\,\mathscr{E}_0^2/8\pi$ gained by reorientation matches the energy expenditure $Kq_1^2/2$ for the "smoothest" of all the possible deformations under the given boundary conditions in the cell. This deformation is characterized by a Fourier component having a minimum (m = 1) value of the wave vector $q_m = m\pi/d$, where m is an integer. The condition $\Delta\epsilon\,\mathscr{E}^2/8\pi = K\pi^2/2d^2$ implies that the threshold voltage for reorientation of the NLC is independent of the thickness of the cell (4).

After we have found by Eq. (3) an expression for the orientation angle of the optic axis $\Theta(z)$ as a function of the field, we find the distribution of the refractive index across the thickness of the cell:

$$n(z) = \frac{n_{\perp} n_{\parallel}}{\sqrt{n_{\perp}^2\cos^2\Theta(z) + n_{\parallel}^2\sin^2\Theta(z)}}, \tag{5}$$

and then we find the phase difference between the ordinary and extraordinary rays $\Phi(\mathscr{E})$ at the exit face of the cell, which depends on the field intensity as a parameter, in terms of $\Theta(z)$:[15]

$$\Phi(\mathscr{E}) = \frac{2\pi}{\lambda}\int_0^d n(z)\,dz = \frac{2\pi d\,\overline{\Delta n(\mathscr{E})}}{\lambda}. \tag{6}$$

The amount of phase retardation determines the intensity of the light transmitted through the cell and analyzer:

$$I = I_0 \sin^2 2\beta \cdot \sin^2\left(\frac{\Phi}{2}\right), \tag{7}$$

Here I_0 is the intensity of linearly polarized light incident on the cell, and β is the angle between the polarization vector of the incident ray and the optic axis of the NLC. Depending on the voltage of the steady-state (d.c. or sinusoidal) electric field, and hence on the phase retardation $\Phi(\mathscr{E})$, the light intensity at the output of the analyzer oscillates. The maximum amplitude of the oscillations corresponds to $\beta = 45°$. Numerical methods of calculation on a computer were used in[14-16,19] to determine the parameters that enter into the problem.

In order to study the transition processes of switching on and off of the deformation effects, we must solve the equation of motion of the director,[20] in which the viscous frictional torque (the left-hand side) is equated to the sum of the dielectric and elastic torques (the case $\mathscr{E} = 0$ has been treated in[15]):

$$\gamma_1 \frac{\partial\Theta}{\partial t} = \frac{\Delta\varepsilon\mathscr{E}^2}{4\pi}\Theta + K_i\frac{\partial^2\Theta}{\partial z^2}; \tag{8}$$

Here K_i is the elastic coefficient, which depends on the boundary conditions for z = 0 and z = d, as in Eq. (4), and γ_1 is the corresponding viscosity coefficient.

When we solve (8), we get expressions for the times of switching on and off of the deformation effects:

$$\tau_{\text{rise}} = \frac{\gamma_1}{(\Delta\varepsilon\mathscr{E}^2/4\pi) - K_i(\pi^2/d^2)} = \frac{4\pi\gamma_1 d^2}{\Delta\varepsilon U^2 - 4\pi^3 K_i}, \tag{9}$$

$$\tau_{\text{decay}} = \frac{\gamma_1 d}{\pi^2 K_i}. \tag{10}$$

Thus the decay time is determined only by the viscoelastic properties of the NLC and the geometry of the layer, while τ_{rise} declines in inverse proportion to the square of the voltage ($U^2 = \mathscr{E}^2 d^2$) when $U^2 > 4\pi^3 K_i/\Delta\epsilon$.

We emphasize that the deformation of a NLC by an electric field does not involve the electric conductivity of the material (the perturbing dielectric moment is proportional to $\Delta\epsilon\mathscr{E}^2$). It has its magnetic analog (the Freedericksz transition), and it does not depend on the frequency of the applied field up to the frequencies of Debye dipole relaxation of the molecules.

2) Experimental data. The most difficult point in the experimental study of the deformation effects is how to fix a definite initial orientation of the molecules of the NLC. It is quite necessary to obtain liquid monocrystals

in studying phase retardation, so as to ensure that Δn will be independent of the coordinates x and y (see Fig. 4b), and also in order to diminish scattering and depolarization of the light. One of the most interesting studies on methods of orienting NLC is [21], which recommends using surface-active organosilicon compounds for getting a uniform orientation of the molecules, both parallel and perpendicular to the electrodes. However, in most cases people establish a parallel orientation by wiping the inside walls of the cell with a cloth.[22] Wiping creates a microrelief on the electrode coating in the form of a system of ridges and grooves, and it is energetically most favorable for the liquid crystal to lie with the molecular axes along the grooves, i.e., in the direction of wiping.[23] The same orientation mechanism also operates when one uses electrode coatings that have been deposited by oblique vacuum evaporation.[24] One can get a perpendicular orientation by chemical treatment of the walls or by mixing certain additives into the NLC.[25]

Experimental data on phase modulation of light using the S-effect in a NLC having $\Delta\epsilon > 0$ are given in[26-28]. In fact, the intensity of the monochromatic light transmitted by the cell oscillates (Fig. 5) as the voltage pulse is switched on and off, in agreement with the theory, owing to reorientation and back-relaxation of the director of the NLC. As was shown in[28], the total change in the phase retardation can amount to 30π (with 15 maxima each at the leading and trailing fronts of the oscillogram), while the voltage sensitivity $\Delta\Phi/\Delta U = \pi/1\,V$. Hence, one can switch on a light beam in certain NLC with a 100% depth of modulation in only 3 μs (with a relaxation time of 250 μs), owing to partial reorientation of the liquid crystal and change of the phase retardation by only π. The corresponding times are 1—2 orders of magnitude greater for NLC that operate at room temperature. Theoretical estimates of the switching time[15] agree qualitatively with experiment.[28,146]

The B-effect in NLC having $\Delta\epsilon < 0$ has been studied in[29-31] in the liquid crystal MBBA or in mixtures based on it. The threshold reorientation voltage agrees well with the value of U_0 found from Eq. (4).[30,31] It does not depend on the thickness of the NLC layer nor on the frequency of the applied field up to hundreds of kilohertz.[29b,30] This agrees with the theoretical predictions.

The T-effect in NLC having $\Delta\epsilon > 0$[32] is of great practical interest because of: a) higher switching contrast as compared with the S-effect, and b) a lower switching threshold as compared with the B-effect. The first advantage arises from the fact that the "phase retardation" upon switching on the field changes from $\pi/2$ to 0 for any thickness of the layer or wavelength of the light, whereas it depends on d and λ in the S-effect (see Eq. (6)). The low threshold voltages arise from the large value of $\Delta\epsilon \approx 10$—$20$[33] of the NLC for which it is positive, whereas usually $|\Delta\epsilon| < 1$ for NLC having $\Delta\epsilon < 0$ (recent information on NLC having $\Delta\epsilon = -2$ to -3[34]

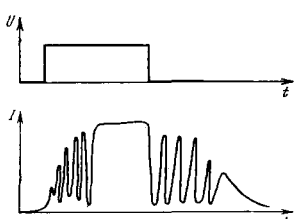

FIG. 5. Variation of the light intensity I transmitted through the layer of NLC having an S-orientation and the analyzer when a voltage pulse U acts on the cell.

constitutes an exception). One can attain $U_0 \approx 1$ V[35] in low-temperature NLC mixtures having $\Delta\epsilon > 0$ over a broad range of frequencies.

The experimentally determined times for complete reorientation and relaxation of the director in the S-, B-, and T-effects are well described by the theoretical relationships (9) and (10), and they are used for determining the corresponding coefficients of elasticity and viscosity of NLC.[15,20,29,146] As we have stated, the switching rate can be increased by a factor of 10—15 for the S- and B-effects by phase modulation of the monochromatic light if $\Delta\Phi \leq \pi$.

b) The electromechanical effect (EME) and ferroelectricity. We have discussed the case in which an electric field deforms a NLC by acting on its dielectric anisotropy $\Delta\epsilon$. Here the dipole moments of the molecules (μ) played only an indirect role in determining the sign of $\Delta\epsilon$. In principle, many of the results of the last section remain in force even when $\mu = 0$. Now we shall discuss an effect caused by a nonzero value of the dipole moment, $\mu \neq 0$, and here the geometric shape of the molecule (wedge- or arc-shaped) proves to be highly essential.

The literature has repeatedly discussed the problem of the incompatibility of the symmetry properties of ordinary NLC with ferroelectricity,[13,36] owing to randomness of orientation of the molecular dipoles in the liquid monocrystal arising from the rotational movement of the molecules (Fig. 6a). However, as Meyer[37] has shown, a polar axis can arise in a liquid monocrystal having wedge-shaped molecules if it is subjected to "transverse bending" deformation (S-deformation), or in a crystal having arc-shaped molecules if the layer is subjected to "longitudinal bending" deformation (B-deformation). Then a polar structure corresponds to denser packing of the molecules (Fig. 6b). Thus, with a certain shape of the molecules, an external deformation gives rise to a charge on the electrodes perpendicular to the polar axis (a piezoeffect). Conversely, an electric field that orients the permanent dipoles causes a deformation of the layer of NLC (an electromechanical effect) that can be detected optically. Figure 6c shows a diagram of the arrangement of the electrodes and the initial orientation of the NLC having $\Delta\epsilon < 0$, while Fig. 6d shows the deformation caused by the electro-mechanical effect (here we are assuming arc-shaped molecules with a direction of the dipole moment as in Fig. 6b).

The curvature of the deformed structure is proportional to the first power of the field $d\Theta/dz = e_{33}\mathcal{E}/K_{33}$, where e_{33} is the piezocoefficient for the given experi-

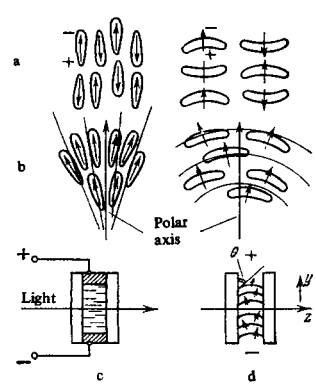

FIG. 6. The electromechanical effect. a) Structure of undeformed NLC having wedge-shaped and arc-shaped molecules; b) the same NLC subjected to S- and B-deformations; c) a cell for observing the EME; d) deformation of a NLC caused by the EME.

mental geometry, and K_{33} is the corresponding elastic coefficient. We note that the B-effect that was discussed above does not occur here, since $\mathcal{E} = \mathbf{L}$, while $\Delta\epsilon < 0$, and the dielectric torque vanishes. The deformation depicted in Fig. 6d leads to birefringence, as is observed experimentally.[38,39] The phase retardation in this case also is proportional to the square of the field, and is determined by the formula[39]

$$\Delta\Phi = \left(\frac{d\Theta}{dz}\right)^2 n_\perp \left(1 - \frac{n_\perp^2}{n_\parallel^2}\right) \frac{d^3}{24}. \qquad (11)$$

The coefficient e_{33} has been determined experimentally for MBBA, whose molecules are arc-shaped. The sign and value of e_{33} agree with the theory.[40] An essential point is that the electromechanical effect does not have a threshold, and it apparently has no frequency limitations up to the Debye relaxation frequency.

A number of studies[41,42] on p-azoxyanisole has observed electrooptical effects that are treated as ferroelectric, namely, an increase in the dielectric constant at very low frequencies (a few hertz or fractions of one hertz), a "ferroelectric" hysteresis loop that can be observed with a classical Sawyer-Tower circuit, domain patterns in polarized light, etc. The ideology in which deformed structures play the major role[38,143] cannot be used in explaining these phenomena. Moreover, a hysteresis loop is observed even in the isotropic phase of this substance,[6,43] while a domain structure is not always correlated with the existence of a loop. It seems to us that such effects arise from a double electric layer at the boundary of the conducting fluid with the electrode. Then the cell has at least a two-layer structure[44], and the decisive role is played by Maxwell-Wagner barrier polarization[45] rather than orientational polarization. This naturally explains the increase in ϵ with decreasing frequency and the formation of a loop (with account taken of the nonlinearity of the volt-ampere curves in pure specimens of p-azoxyanisole).

c) Electrohydrodynamic instability. Domains and light diffraction. The deformation effects in NLC discussed in Sec. a of Chap. 3 arose from the competition of two torques: the dielectric torque $\Delta\epsilon\mathcal{E}^2$ and the elastic torque $K_i q^2$, where q is the wave vector of the deformation (near the reorientation threshold, $q \approx \pi/d$). The electric conductivity of the material was not taken into account here, although in a number of cases (low frequencies, high electric conductivity), anisotropic electric conductivity is precisely the reason for anomalous orientation of NLC by an external field that does not correspond to the sign of the dielectric anisotropy. As a rule, this happens when $\Delta\epsilon < 0$ and $\Delta\sigma > 0$, although cases are known of anomalous orientation when $\Delta\epsilon > 0$ and $\Delta\sigma < 0$.[46] The reason for the anomalous orientation lies in the interaction of the space charge with the external electric field.[47]

Following Helfrich,[48] let us examine a physical model of the appearance of a torque induced by the electric conductivity. Figure 7 shows a slightly deformed (e.g., owing to fluctuations) state of a liquid-crystalline layer that had initially been oriented with the director along the axis Ox. The external electric field $\mathcal{E}_z$ gives rise to a current that has a component I_x owing to the elevated conductivity of the NLC in the x direction. The current I_x leads to partial separation of positive and negative ions along the x direction and to formation of a space-charge field $\mathcal{E}_x$. If we now consider the double layer having the coordinates $x = 0$ and $x = x_a$, we see that

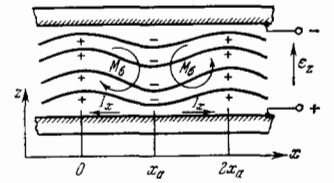

FIG. 7. The model of Helfrich. The solid wavy lines indicate the direction of the director in the slightly deformed liquid crystal.

a torque M_σ arises from its interaction with the field $\mathcal{E}_z$, and it tends to increase the initial deformation. This is resisted by the elastic torque of the NLC and the dielectric torque if $\Delta\epsilon < 0$. The breakdown of the equilibrium of the torques under certain conditions gives rise to electrohydrodynamic (EHD) instability in the form of a periodic pattern of rotational movement of individual regions of the NLC. When $\Delta\epsilon > 0$, the torque M_σ adds to the dielectric torque, and the physical situation differs little from the S-effect described in Sec. a of Chap. 3.

Spatially-periodic patterns of steady-state flow of a substance in an electric field are observed experimentally in polarized light with a NLC having $\Delta\epsilon < 0$ with an orientation of the director $\mathbf{L} \parallel Ox$ (Williams domains[49]). The Williams domains are manifested as a grating (alternation) of dark and light bands when a light beam polarized in the x direction is passed through the specimen, and the bands are perpendicular to the x direction. The threshold voltage for appearance of domains ($U_0 \approx 5$—7 V) does not depend on the thickness of the layer (d), while the grating period is approximately equal to d.

1) Theory of EHD instabilities. In order to determine the threshold for EHD instability of a NLC oriented as shown in Fig. 7, one must solve a system of four linearized equations[50] that describe an incompressible nematic liquid. The first of them, the equation of motion of the director, is analogous to Eq. (8), but it has an additional term $\alpha_2 \partial v_z/\partial x$ on the left-hand side. This term describes the viscous friction torque ($\alpha_2 < 0$ is the coefficient of friction, and v_z is the z component of the velocity of the liquid). In the simplest model in which one treats a steady-state regime ($d\Theta/dt = 0$) while the threshold for the S-effect is high enough (or, equivalently $\epsilon_\parallel \approx \epsilon_\perp = \epsilon$, $\Delta\epsilon \approx 0$), Eq. (8) is simplified:[3)]

$$K_{33}\frac{\partial^2\Theta}{\partial x^2} = \alpha_2 \frac{\partial v_z}{\partial x}. \qquad (12)$$

The second equation describes the movement of the viscous liquid (η is the viscosity) with account taken of the force of the electric field $\mathcal{E}$ acting on the space charge δq (the Navier-Stokes equation). In the simplest case in which the period of the deformations is of the order of the thickness of the layer of NLC ($\lambda_0 \approx d$), we can write this equation as:[130]

$$2\eta \cdot \frac{2\pi}{d}\frac{\partial v_z}{\partial x} = \mathcal{E}\delta q. \qquad (13)$$

The third equation is obtained from the condition of continuity of the current $\operatorname{div} \mathbf{I}_x = 0$, where $I_x = \sigma_\parallel \mathcal{E}_x + \Delta\sigma \cdot \mathcal{E}\Theta$, $\Delta\sigma = \sigma_\parallel - \sigma_\perp$.[52] We get

$$\sigma_\parallel \frac{\partial \mathcal{E}_x}{\partial x} + \Delta\sigma \frac{\partial \Theta}{\partial x} = 0. \qquad (14)$$

And finally, we shall use the Poisson equation

$$\frac{\partial \mathcal{E}_x}{\partial x} = \frac{4\pi}{\varepsilon}\delta q. \qquad (15)$$

We see from (13) that the velocity gradient $\partial v_z/\partial x$ will attain a value at some field value $\mathcal{E}_0$ such that the torque of the frictional forces in Eq. (12) will exceed the elastic

torque. Thus, simultaneous solution of the system (12)–(15) will determine the threshold voltage for instability. Actually,

$$2\eta \cdot \frac{2\pi}{d} \frac{K_{33}}{\alpha_2} \frac{\partial^2 \Theta}{\partial x^2} = \mathcal{E} \frac{\varepsilon}{4\pi} \frac{\partial \mathcal{E}_x}{\partial x} = -\mathcal{E}^2 \frac{\varepsilon}{4\pi} \frac{\Delta\sigma}{\sigma_{\parallel}} \frac{\partial \Theta}{\partial x}. \qquad (16)$$

If we assume that $\partial^2\Theta/\partial x^2 \approx (2\pi/d)\partial\Theta/\partial x$, then because of the condition $\lambda_0 \approx d$ (periodic deformation [130]), we get the following expression for the threshold voltage for instability:

$$U_0^2 = \frac{32\pi^3 K_{33}\eta\sigma_{\parallel}}{(-\alpha_2)\varepsilon\Delta\sigma}. \qquad (17)$$

The qualitatively-derived Eq. (17) does not differ in principle from the more exact expression given in [50]. Numerical estimates give a value of the order of 10 V, which agrees satisfactorily with experiment. The solution of the problem obtained by Helfrich [48] that takes account of the dielectric anisotropy of the NLC, $\Delta\epsilon = \epsilon_{\parallel} - \epsilon_{\perp} < 0$, gives a somewhat more complex formula for the threshold voltage (the case $\mathbf{L} \parallel Ox$; see Fig. 7):

$$U_0^2 = \frac{4\pi^2 K_{33}}{\Delta\varepsilon(\sigma_{\perp}/\sigma_{\parallel}) + (k_1/\eta_1)\varepsilon_{\parallel}[(\varepsilon_{\perp}/\varepsilon_{\parallel}) - (\sigma_{\perp}/\sigma_{\parallel})]}. \qquad (18)$$

An analogous expression is given in [48] for $\mathbf{L} \perp Ox$, but with different coefficients of elasticity, friction, and viscosity (k_{11}, k_2, and η_2, respectively). Formally, Eq. (18) is reduced to (17) when $\Delta\epsilon = 0$.[4)]

The theory of [48] has a substantial defect. It does not take account of the boundary conditions, while, as we have stated, the wave vector of the spatial deformations in the x direction (q_x) was assumed to be equal to π/d. The steady-state problem with account taken of the boundary conditions has been solved independently in [50,51]. Here the solution of even the linearized problem required a computer. The rigorous expressions for U_0 that were derived in [51], and which depend parametrically on the ratio of wave vectors $s \equiv q_z/q_x$ are formally reduced for $s = 0$ to Eq. (18). In fact, the meaning of the viscosity coefficients in Eq. (18) proves to differ with different authors, [47,51,52] and it is apparently given most correctly in [51]: $k_1 = \alpha_2$, $k_2 = \alpha_3$, $\eta_2 = (-\alpha_2 + \alpha_4 + \alpha_5)/2$, $\eta_1 = (\alpha_3 + \alpha_4 + \alpha_6)/2$, where the α_i are the coefficients of Leslie. [53]

For the case $s \neq 0$, according to rigorous numerical calculations, [50,51] the wave vector q_x proves to be a function of the voltage U, but not in a single-valued way. There are several dispersion curves that relate q_x and U (see Fig. 8a, which qualitatively illustrates the results of [51] for the liquid crystal MBBA). Instability does not arise at low voltages $U < U_{01}$, while at $U = U_{01}$ (6.9 V for MBBA) a deformation pattern arises with the period $W \approx 2d$ (branch 1 in Fig. 8a). This corresponds to steady-state rotational movement of the NLC as depicted in Fig. 8b. The numerical value of the threshold voltage U_{01} is higher than U_0 from Eq. (18); for any orientation of the director $\mathbf{L} \parallel Ox$ and $\mathbf{L} \perp Ox$, all the parameters k_1, k_2, η_1, η_2, K_{33}, and K_{11} simultaneously enter into U_{01}.

The period W does not vary upon further voltage increase ($U_{01} < U < U_{02}$). In the opinion of the authors of [51], this regime corresponds to the lower branch of curve 1 in Fig. 8a (Williams domains). When $U = U_{02}$ (U_{02} = 13 V for MBBA)., the type of vortex movement changes from that depicted in Fig. 8b to that depicted in Fig. 8c, i.e., the period of the vortices is cut in half. Further voltage increase, according to the linearized theory, gives rise to 3- and 4-layer vortex patterns, etc. One gets an analogous pattern also in the case of a perpendicular initial orientation of a NLC having $\Delta\epsilon < 0$

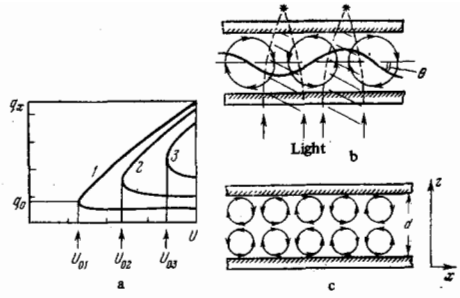

FIG. 8. Illustration for the linear theory of EHD instability of NLC. a) Dispersion curves $q_x(U)$ for $\mathcal{E} \perp \mathbf{L}$ (q_x is the wave vector of the deformation, and U is the external voltage); b) the type of vortical movement of the NLC corresponding to curve 1 of $q_x(U)$ (Θ is the angle of inclination of the director to the axis Ox, and the asterisks indicate the bright lines of the domains when the NLC layer is illuminated from below); c) the type of vortical movement corresponding to curve 2 of $q_x(U)$.

(see Fig. 4c), with only the difference that the B-effect can occur first, as was discussed in Sec. a of Chap. 3 (e.g., the threshold of the B-effect for MBBA is lower than the threshold of EHD instability [51b]).

The behavior of a NLC in an alternating field ($\omega \neq 0$) has been treated theoretically in [52] (without taking account of the boundary conditions). The relation of the instability threshold to the frequency of the external field for $\omega < \omega_c$ and to the geometry of Fig. 7 is given by the following expression

$$\overline{U_0^2(\omega)} = \frac{U_0^2(1+\omega^2\tau_0^2)}{\xi^2 - (1+\omega^2\tau_0^2)}, \qquad (19)$$

Here $\overline{U_0^2(\omega)}$ is the mean-square value of the threshold voltage at the frequency ω, U_0 is determined from Eq. (18), or, according to the more exact theory, [50,51] the critical frequency $\omega_c = (\xi^2 - 1)^{1/2}/\tau_0$ is defined in terms of the time of dielectric relaxation $\tau_0 = 4\pi\epsilon_{\parallel}/\sigma_{\parallel}$ (the relaxation time of the space charge along the x axis), while the parameter $(\xi^2 - 1)$ contains only the constants of the material, and is equal to the product of the quantity $(-\epsilon_{\parallel}/\Delta\epsilon \cdot \epsilon_{\perp})$ by the denominator in Eq. (18).

Equation (19) implies that the threshold voltage of EHD instability sharply increases as $\omega \to \omega_c$. Let us explain the physics of this phenomenon. Although the ionic current along the axis Oz (see Fig. 7) follows the external field without lag, the process of space-charge separation along the x coordinate lags in phase behind the field with increasing frequency. This diminishes the force exerted on the space charge q by the external field $\mathcal{E}$ (the d.c. component of the product $q_m \mathcal{E}_m \cos(\omega t) \times \cos(\omega t - \varphi)$ is decreased). The torque M_σ is decreased, and one must increase the external voltage to attain instability.

While at frequencies $\omega < \omega_c$ (conduction regime), the threshold voltage does not depend on the thickness of the layer of NLC, an instability regime is established for $\omega > \omega_c$ for which the threshold field intensity does not depend on the thickness (dielectric regime). In this regime, $U_0^2(\omega) \sim d^2\omega$, and the wave vector of the deformation pattern depends on the frequency, $q_x \sim \sqrt{\omega}$. According to [52], the calculation of the instability threshold in the dielectric regime is complicated, and it requires computer technique. A simple expression has been proposed in [56] for the threshold field in the frequency region $\omega > \omega_c$, ω_0, where $\omega_0 \approx \beta\pi^2/d^2\rho$ (ρ is the density of the material, and β is a combination of the viscosity coefficients of Leslie, $\beta = (\alpha_3 + \alpha_4 + \alpha_6)/2$):

$$\overline{\mathcal{E}_0^2(\omega)} = \overline{d^2 U_0^2(\omega)} \approx \frac{8\alpha_2\omega}{\Delta\varepsilon}. \qquad (20)$$

Rather simple expressions for $\overline{\mathcal{E}_0^2(\omega)}$ are given in [56] for the frequency range $\omega_c < \omega < \omega_0$ that are intermediate in their meaning between those given by Eqs. (19) and (20). Figure 9 illustrates qualitatively the theoretical variation of $\overline{U_0^2(\omega)}$ for two thicknesses of the NLC layer (d_1, and $d_2 = 3d_1$).

The time characteristics of the appearance and disappearance of instabilities as the field is switched on and off are described in their general features by Eqs. (9) and (10), with only the difference that the term that contains $\Delta\epsilon$ in (9) is multiplied by the factor $\epsilon_\perp/\epsilon_\parallel$, [52] which accounts for the transverse field $\mathcal{E}_x$ in Fig. 7.

2) Experimental data. We have discussed the theory of appearance of instabilities caused by the type of anisotropy of the liquid. The fundamental conclusions of the theory have been well confirmed by experiment: [145]

a) Williams domains (low-frequency EHD instability) actually appear only in a NLC having $\Delta\epsilon < 0$ [12,57] that has a sufficient electric conductivity. [58] An exception to this is [46b] where they observed Williams domains in an alternating current and dynamic scattering in butoxybenzoic acid, which has a small positive anisotropy in the nematic phase. This might involve the fact that the criterion $\Delta\epsilon < 0$ is approximate in nature, [59] while the exact criterion must be found from the exact expression for the threshold voltage in line with the theory. [50,51] The study [51b] was concerned with theoretical study of EHD instabilities of NLC having $\Delta\epsilon > 0$ with direct current.

b) It has been experimentally possible to establish the vortex nature of the movement of the liquid, as shown in Fig. 8b, by observing solid particles mixed into the NLC, and even to measure the velocity of this movement (tens of μm/sec) as a function of the voltage. [61] The vortex movement partially orients the NLC, especially strongly in the region of maximum velocity gradient, i.e., at the centers of the vortices. This leads to the periodic variation of the orientation of the director shown in Fig. 8b by the solid line, which in turn causes a periodic variation of the refractive index for light polarized along the Ox axis. The grating of cylindrical lenses thus formed [60] focuses the transmitted beam into bright lines, which are the Williams domains.

c) The period of the Williams domains is proportional to the thickness of the layer, it does not depend on the frequency, and it depends weakly on the amplitude of the external voltage. [60,62]

d) The frequency dependence of the instability threshold is described by Eqs. (19) and (20), although the experimental value of the critical frequency does not always agree with the calculated value. [52a, 58, 62] The numerical value of U_0 ($\omega \to 0$) agrees well with the theory (see the estimates for MBBA and p-azoxyanisole in [50,51]).

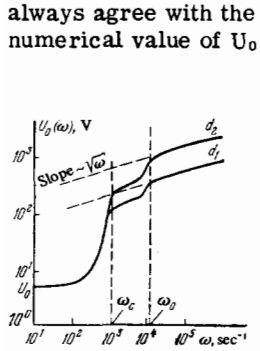

FIG. 9. Frequency-dependences of the threshold voltage of EHD instability for NLC layers of thicknesses d_1 and $d_2 = 3d_1$.

e) The times for appearance of instability and for relaxation of the deformation pattern are described by Eqs. (9) and (10). This makes it possible to determine the viscosity coefficients experimentally. [58]

f) One observes a specific form of instability at frequencies $\omega > \omega_c$ (the so-called "chevrons" [63]). As the theory implies, their period is considerably shorter than that of the Williams domains, it does not depend on the thickness of the layer, and it varies with increasing voltage, [63b] while the deformation pattern itself oscillates with the frequency of the field. [64] In thin, poorly-conducting specimens ($\omega_c \to 0$), one observes a domain pattern having a period that declines in inverse proportion to the voltage at low frequencies, and even does so with direct current. [54,55]

Since the domain structure is a grating having a periodic variation of the refractive index, a distinct diffraction pattern arises on the screen when light of wavelength λ and polarization vector e $\parallel$ L is transmitted through the structure. The maxima and minima are distributed along a line parallel to the director. [65,66] The angular distribution of the maxima is described by the usual formula for a diffraction grating of period W:

$$W \sin \xi = m\lambda \qquad (m = 0, 1, 2, \ldots). \qquad (21)$$

It is hard to change the period of the grating if it is formed of Williams domains (see [66]), but one can get a smooth control of the deviation angle of the beam by using the domains described in [54,55].

We should make a comment here. As a rule, the experimental data agree well with the theory of EHD instabilities based on the Helfrich mechanism when one uses an alternating field. Another mechanism of EHD instability arises in a d.c. field, where injection phenomena are important. This mechanism is not specific for liquid crystals, but is manifested in any poorly-conducting liquids. The movement of a liquid that involves injectional EHD instability is most easily observed in NLC, owing to the anisotropy of their optical properties, and it often masks the Helfrich instability. The theory of the threshold for injectional instability for the case of monopolar injection [67,130] gives values of U_0 that appreciably exceed the experimental values. [62,63] The agreement between theory and experiment is quite satisfactory if one accounts for bipolar injection. [68] In particular, one can explain by the injection mechanism the periodic movement of the liquid in the isotropic phase of p-azoxyanisole, [69] and the domains [59] and light diffraction [70] in NLC having $\Delta\epsilon > 0$.

d) Dynamic light scattering. According to the linearized theory of Pikin and Penz, [50,51] a new regime of instability sets in at some voltage above the threshold $U = U_{02} > U_{01}$ in NLC having $\Delta\epsilon < 0$. It is characterized by two-layer vortex movement (see Fig. 8c), and then three-layer movement at $U = U_{03} > U_{02}$, etc. These layer separations are not observed in real NLC because of the nonlinearity of the deformations, but a turbulent movement of the liquid sets in that is accompanied by intense scattering of the transmitted light. [10,71,72] It has been termed dynamic scattering (Fig. 10a). There is as yet no rigorous nonlinear theory of the response of a liquid-crystalline system to an external electric field, although a qualitative treatment of the turbulent movement has been given in [73], while the relationship be-

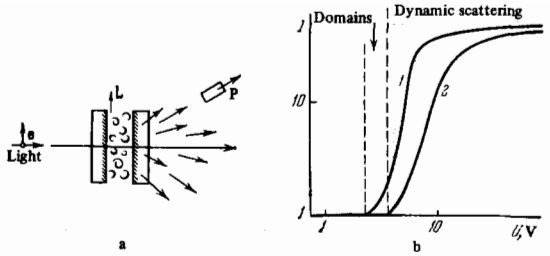

FIG. 10. Dynamic light scattering. a) Diagram of the experiment (P is the photodetector); b) the intensity of scattered light as a function of the voltage applied to the cell: curve 1 is for the case $\mathbf{e} \parallel \mathbf{L}$, and curve 2 for $\mathbf{e} \perp \mathbf{L}$ (e is the polarization vector of the light, and L is the director of the NLC).

tween the spatial distribution of the director and the voltage has been obtained in [74] (see Fig. 8b) in the region of large angles Θ (to an accuracy of third-order terms in Θ). However, the transition from a regular pattern of one-dimensional diffraction to a practically isotropic cone of scattered light (mainly in the forward direction) physically arises from the subdivision of the regular banded domain structure into turbulent vortices of all possible shapes with a broad spectrum of wave vectors q_x and q_y.

The more or less uniform distribution of deformations over the wave vectors, in line with the law of conservation of momentum in the theory of light scattering, [75] leads to a broad range of scattering angles ξ (cf. Eq. (15)):

$$q = 2\frac{\omega'}{c}\sin\frac{\xi}{2}. \qquad (22)$$

In Eq. (22), ω' and c are the frequency and velocity of the light incident on the cell, respectively. The intensity of dynamic scattering is practically independent of the direction of polarization of the light and of the initial orientation of the NLC layer (Fig. 10b).

A large number of experimental studies have been devoted to the dynamic-scattering effect, in view of its practical importance. The contrast characteristics of the scattering have been studied in [76,77], and the time characteristics in [72,77]. It has turned out that the times for switching on and off of dynamic scattering are close to the corresponding values for domain instability, except for the region of secondary dynamic scattering, where the relaxation times are substantially prolonged. [58,78] The studies [79] were concerned with the dependence of the d.c. threshold for dynamic scattering on the impurity composition of a NLC in terms of a mechanism of injectional instability. It was shown possible in [144] to increase appreciably the a.c. scattering threshold of a NLC (from 5 V to 9 V) by reducing the anisotropy of the electric conductivity $\sigma_\parallel/\sigma_\perp$ from 1.4 to 1.15, which confirms the theory. [48,50]

In concluding this section, we shall give a summary of the electrooptical effects that are most characteristic of NLC (Table I).

TABLE I. Electrooptical effects in NLC

Dielectric anisotropy	$\Delta\varepsilon > 0$		$\Delta\varepsilon < 0$			
Electric conductivity	$\sigma = 0, \neq 0$		$\sigma = 0$		$\sigma \neq 0$	
Orientation	$\mathbf{L} \parallel \mathcal{E}$	$\mathbf{L} \perp \mathcal{E}$	$\mathbf{L} \perp \mathcal{E}$	$\mathbf{L} \parallel \mathcal{E}$	$\mathbf{L} \perp \mathcal{E}$	$\mathbf{L} \parallel \mathcal{E}$
$\omega \neq 0$; direction of increasing field ↓	S or EME for wedge-type molecules	S- and T-deformation; phase modulation of light (*)	S or EME for arc-type molecules	B-deformation; phase modulation of light (*)	Periodic deformation owing to EHD instability ($\omega < \omega_c$ – WD; $\omega > \omega_c$ – chevrons); light diffraction Turbulent movement; dynamic light scattering	B-deformation; phase modulation of light (*)
$\omega = 0$	Injectional instability; diffraction and scattering of light.					

Notation: S–stability, EME–electromechanical effect, WD–Williams domains. The asterisks indicate the effects that have magnetic analogs.

4. ELECTROOPTICS OF CHOLESTERIC LIQUID CRYSTALS

We have already stated (Chap. 1) that the director L of a CLC describes a helix in space having the pitch p (rotation of L through the angle 2π). The axis h of the helix lies perpendicular to the long molecular axes, i.e., $\mathbf{h} \perp \mathbf{L}$. The nature of the electrooptical behavior of a CLC depends substantially on the orientation of the axis of the helix with respect to the electrodes of the cell, as depicted in Fig. 4a. We should distinguish the two most important cases of orientation of a CLC, or as they say, the two textures: planar and focal-conic. [1,81]

One can impart the planar texture by special treatment of the electrode coatings, with subsequent slow cooling of the material from the isotropic phase, and also by an electric or magnetic field. [82] Here the axes of the molecules are parallel to the electrode surface, while the axis of the helix is perpendicular to the electrodes (the field $\mathcal{E} \parallel \mathbf{h}$). This orientation is analogous to the T-orientation of a NLC (see Fig. 4d), but while 1/4 of a turn fits into the thickness d of a cell for the NLC ($d = p/4$), [83] the relationship $d \gg p$ holds for a CLC. In agreement with the theory, [84] the planar texture is optically active, and the rotation of the plane of polarization of the light is as much as 10^4–10^5 deg/mm thickness of the layer. Moreover, this texture selectively reflects circularly-polarized light whose sign of rotation of the polarization vector agrees with the sign of rotation of the helix, provided that the wavelength in the medium $\lambda_0 \approx p/2$. This selective reflection is due to light diffraction by the equidistant planes of the CLC having identical refractive indices, by analogy with the Bragg diffraction of X-rays by a crystal lattice.

By using a magnetic field [85] in relatively thick cells (100 μm or more), or with an electric potential for CLC having a positive dielectric anisotropy, one can attain an orientation in which the axis of the helix lies parallel to the electrode in one direction (e.g., x), or these axes are directed at random in the xy plane in individual regions of the layer of CLC, but always perpendicular to the axis Oz. In contrast to the planar texture, this texture (focal-conic) strongly scatters light, and the scattering is selective as a function of λ. [86] For a focal-conic texture, $\mathcal{E} \perp \mathbf{h}$, and there is a certain resemblance between the electrooptical properties of a CLC and the properties of a NLC having an initial B-orientation (see Fig. 4c).

Both nematic and cholesteric liquid crystals are characterized by a certain anisotropy, electric ($\Delta\epsilon = \epsilon_\parallel - \epsilon_\perp$, $\Delta\sigma = \sigma_\parallel - \sigma_\perp$), and optical ($\Delta n = n_\parallel - n_\perp$).

Here the subscripts $\parallel$ and $\perp$ denote the directions parallel and perpendicular to the director **L**, rather than the axis h of the helix. However, if we introduce the quantities $\epsilon_{\parallel h}$ and $\epsilon_{\perp h}$ (and $\sigma_{\parallel h}$ and $\sigma_{\perp h}$ for the components of the electric conductivity), respectively parallel and perpendicular to the helical axis, then the following relationships[87] hold for a CLC:

$$\varepsilon_{\parallel h}=\varepsilon_{\perp},\ \varepsilon_{\perp h}=\tfrac{1}{2}(\varepsilon_{\parallel}+\varepsilon_{\perp}),\ \sigma_{\parallel h}=\sigma_{\perp},\ \sigma_{\perp h}=\tfrac{1}{2}(\sigma_{\parallel}+\sigma_{\perp}). \quad (23)$$

The inequality $\sigma_{\parallel} > \sigma_{\perp}$ holds in all known CLC, but substances differ in having positive ($\epsilon_{\parallel} > \epsilon_{\perp}$, $\epsilon_{\parallel h} < \epsilon_{\perp h}$) and negative ($\epsilon_{\parallel} < \epsilon_{\perp}$, $\epsilon_{\parallel h} > \epsilon_{\perp h}$) dielectric anisotropy, and the nature of the electrooptical effects depends substantially on the sign of $\Delta\epsilon$.

The study of the electrooptics of CLC began relatively recently,[88] and we have as yet neither a sufficiently rationalized classification of the phenomena, nor a fixed terminology. We shall try below to give a full list of the currently known electrooptical effects in CLC, by classifying the substances in terms of the sign of dielectric anisotropy and the type of initial texture (planar or focal-conic). Here we shall first treat the chronologically earliest studied case of liquid crystals having $\Delta\epsilon > 0$.

a) CLC with $\Delta\epsilon > 0$. The situation is simplest when $\Delta\epsilon > 0$, and the initial orientation is focal-conic. When an electric field exceeding $\mathscr{E}_0^{C\to N}$ is applied to the specimen, a phase transition from a cholesteric to a nematic phase occurs. One can calculate the value of the threshold field by starting with an expression for the free energy of the substance in an electric field analogous to Eq. (3), but with account taken of the helical structure of the CLC:[89]

$$\mathscr{E}_0^{C-N}=\frac{\pi^2}{p_0}\sqrt{\frac{4\pi K_{22}}{\Delta\varepsilon}}; \quad (24)$$

Here p_0 is the pitch of the helix in the absence of a field, and K_{22} is the modulus of rotational elasticity.

We note the close analogy of Eqs. (24) and (4). For the reorientation of a NLC, the threshold field intensity corresponded to an elastic deformation with the minimum wave vector $q_1 = \pi/d$, where d is the thickness of the layer. For the same reason, a field intensity is required for unwinding a CLC helix of pitch p_0 such that the electrostatic energy suffices for elastic deformation with a wave vector $q_0 \approx \pi/p_0$. In contrast to (4), where U_0 corresponds to onset of deformation of the layer, Eq. (24) describes the threshold for complete unwinding of the helix. Hence the appearance of the additional coefficient π in (24) is not remarkable. The phase transition CLC → NLC experimentally observed in[90] is preceded by a voltage region where one observes a gradual unwinding of the helix accompanied by a shift in the peak of the scattered light to longer wavelengths in the spectrum. The cell becomes completely transparent in fields above $\mathscr{E}_0^{C\to N}$ (the case of a NLC having a perpendicular orientation).

Equation (24) has been confirmed in[91], where they used it to determine the coefficient K_{22} for a mixture of cholesterol esters. It was shown in[92] that the threshold field does not depend on the frequency up to the Debye relaxation frequencies of the dipole molecules. In pure CLC (p_0 small), the threshold fields are of the order of $\mathscr{E}_0^{C\to N} \approx 10^5$ V/cm. In mixtures of cholesteric with nematic crystals, which we should also classify as being cholesteric, the helical pitch is substantially greater than in pure CLC. Hence the phase-transition threshold is lowered. This makes it possible to apply this effect for practical purposes (elimination of the characteristic scattering of a CLC by using an electric field[93]). Nematic-cholesteric mixtures having a high, positive $\Delta\epsilon$ have been studied in detail in[94], where they showed that the threshold voltage $U_0^{C\to N}$ is proportional to the thickness d of the cell ($\mathscr{E}_0^{C\to N} = U_0^{C\to N}/d \approx 5 \times 10^4$ V/cm), and they determined the times for back-relaxation from the transparent state (NLC) to the opaque state (CLC), $\tau_{decay} \approx 0.1$ sec. According to the data of[91], the relaxation times for partial unwinding of the helix are of the order of milliseconds.

We note that the phase transition CLC → NLC is observed only when $\Delta\epsilon > 0$,[95] and it has its magnetic analog.[89,96]

The planar texture is less stable than the focal-conic when $\Delta\epsilon < 0$, especially for nematic-cholesteric mixtures having a long helical pitch. In this case, the theory predicts appearance of spatially-periodic deformations of the liquid crystal, with a threshold field that depends on the geometry of the cell. These deformations must occur both in the absence[97] and the presence[87] of conductivity. The simplest of the instabilities is the dielectric one, whose cause is analogous to that treated for the case of S-deformation of a NLC having $\Delta\epsilon > 0$ (see Sec. a of Chap. 3). At a certain value of the field intensity ($\mathscr{E}_0^2$), the energy of dielectric polarization proves to equal the elastic energy of the CLC. The square of the threshold field intensity depends on the pitch p_0 of the helix and the thickness d of the layer of CLC. In the case where $p_0 \ll d$, it is determined by their geometric mean[97,5] (cf. Eqs. (4) and (24)):

$$(\mathscr{E}_0^{\varepsilon})^2 \sim \frac{\varepsilon_{\perp h}}{\varepsilon_{\parallel h}(\varepsilon_{\perp h}-\varepsilon_{\parallel h})}\frac{1}{p_0 d}. \quad (25)$$

A numerical estimate of the threshold voltage in NLC–CLC mixtures where $p_0 \sim 0.1$ d gives a value $U_0^{\varepsilon} \approx 8\sqrt{d/p_0} \approx 20$–$30$ V.

Material flows do not arise in a CLC in the absence of conductivity, and the deformation pattern is purely static in type. When the conductivity of the liquid crystal is sufficient, a space charge can be induced. This leads to vortical movement of the liquid, with concomitant light scattering. This is an electrohydrodynamic instability analogous to the above-studied EHD instability of a NLC.[48] The expression for the threshold field for EHD instability of a CLC for direct current ($\mathscr{E}_0^{\sigma}$), as derived in[87], is analogous to Eq. (25), but with $\epsilon_{\perp h}$ and $\epsilon_{\parallel h}$ replaced by the corresponding quantities $\sigma_{\perp h}$ and $\sigma_{\parallel h}$.

Since the field $\mathscr{E}_0^{\sigma}$ is proportional to the factor $(p_0 d)^{-1/2}$, the instability threshold is evidently substantially lower in nematic-cholesteric mixtures having a large helical pitch than in pure CLC.

Periodic deformations (a cellular deformation pattern) have been observed experimentally in[98] in mixtures of cholesterol esters, and they found qualitative agreement with the theory of Helfrich[87] for the relation of the spatial period W of the pattern to the thickness of the cell (over the range 6–80 μm) and to the helical pitch (over the range 380–660 nm):

$$W^2 = p_0 d\sqrt{\frac{2K_{33}}{K_{22}}}. \quad (26)$$

They also determined in[98] the relaxation time of the

cellular structure after the voltage on the electrodes had been turned off, $\tau_{decay} \approx 50\ \mu$sec.

The dependence of the threshold field on $p_0 d$ was confirmed in [99,147] with nematic-cholesteric low-temperature mixtures. The frequency-dependences of the threshold field intensity $\mathscr{E}_0^{\sigma}(\omega)$ are described by Eq. (27), which was theoretically derived by Hurault [100] by analogy with the treatment of a NLC in [52]:

$$[\mathscr{E}_0^{\sigma}(\omega)]^2 \sim \frac{1+\omega^2\tau_0^2}{1-\zeta^2+\omega^2\tau_0^2}; \qquad (27)$$

Here $\tau_0 = (\epsilon_{\parallel} + \epsilon_{\perp})/4\pi(\sigma_{\parallel} + \sigma_{\perp})$ is the dielectric relaxation time, and $\zeta^2 = 1 - [(\epsilon_{\parallel} + \epsilon_{\perp})/\Delta\epsilon][\Delta\sigma/(\sigma_{\parallel} + \sigma_{\perp})]$. Equation (27) predicts saturation of the threshold field with increasing frequency in the region $\omega\tau_0 \gg 1$, as has been observed experimentally. [99] There is a magnetic analog for pure dielectric instability ($\sigma = 0$); [97,101] EHD instability has no magnetic analog.

The periodic deformation patterns discussed above do not always arise. The threshold of these instabilities for thin CLC layers having a short helical pitch (small product $p_0 d$) and small value of $\Delta\epsilon$ can be so high that other effects supervene upon increasing the field intensity. Thus, certain studies [88,102] have observed a shift of the maximum of selective reflection to shorter wavelengths. This blue shift of λ_{max} must occur if the electric field contracts the cholesteric helix, as predicted by Meyer for the case $K_{22} < K_{33}$ [89] (the so-called conical deformation). Indeed, one cannot reconcile the experimental and theoretical results. [86] A completely different explanation is given in [103] for the blue shift, which can involve imperfections in the planar texture, individual regions of which are differently oriented, and which have a different threshold for periodic instability. Consequently, different regions successively cease to contribute to reflection as the field increases, thus giving an apparent blue-shift effect. The times for relaxation and reaction of the blue-shift effect and the possibility of lowering them to a value of the order of 0.1 sec have been studied in [104].

The blue shift is observed in fields of $(2-5) \times 10^4$ V/cm. Upon further increase in the field intensity, the axis of the cholesteric helix rotates by 90° (in line with the sign $\Delta\epsilon > 0$), and the planar texture is converted into focal-conic. [105,106] The subsequent behavior of the CLC with increasing field does not differ from the case in which a focal-conic texture had existed from the outset. That is, a phase transition of the CLC to a NLC occurs with the threshold field defined by Eq. (24).

b) CLC with $\Delta\epsilon < 0$. Here the focal-conic texture is to some extent analogous to a NLC having $\Delta\epsilon < 0$ with an initial perpendicular orientation. Application of an electric field to the electrodes rotates the helical axis by 90°, and the focal-conic texture is converted into a planar one (analogously to the B-effect in a NLC). Here the liquid-crystal film goes from a scattering to a transparent, optically-active state. This effect was first observed in [107] in nematic-cholesteric mixtures (erasure of scattering), while an interpretation of the phenomenon using ideas of the transition of the one texture into the other is given in [108]. When the CLC is conductive, EHD effects can occur with a focal-conic texture. Hence one usually observes the transition to a planar structure at a relatively high frequency ($\omega > \omega_c \sim 10^3$ Hz). [107,108a] Here the reorientation threshold of nematic-cholesteric mixtures is proportional to the frequency and to the concentration of the cholesteric component, i.e., to $1/p_0$. It was shown in [109] that the critical frequency that converts the scattering state of the film that is characteristic of a focal-conic texture into a transparent state (planar texture) is proportional to the electric conductivity, and it is determined by the dielectric relaxation time of the material $\tau_0 \approx 4\pi\sigma/\epsilon$.

The planar texture is stable with respect to purely dielectric perturbations. However, just as with a CLC having $\Delta\epsilon > 0$, EHD instability can arise in substances having a negative dielectric anisotropy if their electric conductivity is high enough. [87] As has been shown in [95,110], the sign of $\Delta\epsilon$ is of no significance in determining whether EHD instability will arise in CLC. The d.c. threshold field when $\Delta\epsilon < 0$ increases with decreasing helical pitch, [111] and it is given by the same expressions as when $\Delta\epsilon > 0$. The threshold voltage increases with increasing frequency, and in full analogy with NLC having $\Delta\epsilon < 0$, there are two regimes: a conduction regime and a dielectric regime. [99b] In the conduction regime ($\omega < \omega_c$), the threshold voltage increases as we approach the critical frequency ω_c, which depends on the electric conductivity (cf. Eq. (19)). In the dielectric regime ($\omega > \omega_c$), the threshold field is proportional to $\sqrt{\omega}$, just as for a NLC. [99b]

EHD instability in nematic-cholesteric mixtures having $\Delta\epsilon < 0$ gives rise to vortical movement of the liquid, with complete breakdown of the original planar texture. This disturbed structure that strongly scatters light persists after the voltage has been removed from the electrodes. Thus, the entire phenomenon looks like dynamic scattering "with memory". [107] Analogous effects are also observed in purely cholesteric mixtures. [112]

As was shown in [108], the residual scattering is due to transition of the CLC from a planar to a focal-conic texture owing to the vortical movement of the liquid, rather than to formation of an emulsion. [107] The time of existence of the focal-conic texture, i.e., the memory time, depends exponentially on the ratio of the cell thickness to the pitch of the cholesteric helix:

$$\tau_{decay} = Ae^{-Bd/p_0}, \qquad (28)$$

and it varies from one minute to several days in the range of d/p_0 from 2 to 15 [113] (A, B = const.).

Table II summarizes all of the electrooptical effects in CLC. Here the substances are classified according to the sign of the dielectric anisotropy and the type of initial texture, focal-conic (FCT) or planar (PT).

5. OTHER EXAMPLES OF ELECTROOPTICAL EFFECTS

a) Smectic liquid crystals. As compared with NLC, smectic liquid crystals have a higher degree of orientational order, and correspondingly, a higher anisotropy of the dielectric constant. In different substances, the latter can be either negative [48b, 114] or positive. [115,116] However, owing to the high viscosity and strong adhesion to the bounding surfaces, SLC are difficult to orient by an external field. [117] Thus, while a magnetic field of 10–15 kilogauss suffices to incline the molecules within a smectic layer (Fig. 1c), [116,118] field of 60 kilogauss or more are needed to reorient the smectic planes. [116]

The ability of a SLC to be oriented by an electric field was established as early as the thirties. [119] Recently, Carr [115,116] has studied in detail the orientation of var-

TABLE II. Electrooptical effects in CLC*

$\Delta\varepsilon$	$\Delta\varepsilon > 0$, $\varepsilon_{\parallel h} < \varepsilon_{\perp h}$		$\Delta\varepsilon < 0$, $\varepsilon_{\parallel h} > \varepsilon_{\perp h}$	
Texture	FCT, $\mathcal{E} \perp$ h	PT, $\mathcal{E} \parallel$ h	FCT, $\mathcal{E} \perp$ h	PT, $\mathcal{E} \parallel$ h
$\mathcal{E}$ ↓		Periodic deformation owing to dielectric ($\sigma \approx 0$) (*) or EHD instability ($\sigma \neq 0$)		S for $\sigma = 0$
	Untwisting of the helix (*)	"Blue shift" of λ_{max} (*)	EHD instability; dynamic light scattering	
	CLC → NLC phase transition (*)	Rotation of the helical axis by 90° and transition to a FCT (*)	Rotation of the helical axis and transition to a PT ("erasure" of scattering) (*)	Formation of a FCT owing to movement of the material ("memory")
		Phase transition to a NLC when $K_{22} > K_{33}$ (*)		

*) See Table I for notation.

ious SLC in audiofrequency electric fields. He showed that SLC are oriented by the field at frequencies above the critical ($\omega > \omega_c \sim 1/\tau_0$, where τ_0 is the dielectric relaxation time) in accord with the sign of their dielectric anisotropy. Anomalous orientation often occurs at low frequencies ($\omega < \omega_c$) that are caused by the anisotropy of the electric conductivity $\Delta\sigma = \sigma_{\parallel} - \sigma_{\perp}$. As a rule, $\Delta\sigma < 0$ in SLC, owing to the higher mobility of the charge carriers along the smectic planes, i.e., perpendicular to the director **L**. Thus, if the electric conductivity is high enough, low-frequency and d.c. fields orient SLC with the long molecular axes perpendicular to the field, independently of the sign of $\Delta\epsilon$.

The threshold field for appearance of domain instability in a SLC (~7000 V/cm) is about an order of magnitude higher than the instability threshold of the same liquid crystal in the nematic phase, while the period of the domains is substantially smaller. One observes turbulent movement in the SLC with increasing voltage that is accompanied by intense light scattering.[120] A decrease in light transmission in a SLC in an electric field was observed in[121], and it persisted after removing the voltage from the electrodes.

The theory of electrohydrodynamic instabilities of SLC has been treated in[122] within the framework of Helfrich's idea,[48] but with account taken of the firm connection of the director with the smectic layers and the inequality $\Delta\sigma < 0$. The obtained frequency-dependence of the instability threshold is analogous to the corresponding result for a NLC[52] in the limit $\gamma_1 \to \infty$, where γ_1 is the viscosity coefficient. It does not yet seem possible to compare the theory with experiment, since no systematic studies have yet been conducted on the frequency behavior of SLC in an electric field, and moreover, there are not enough data on the physical parameters of these substances (viscosity, elasticity, dielectric constants, electric conductivity, etc.). There is also a serious difficulty in getting a given uniform orientation of a SLC in an electrooptical cell. There is a single study[123] in which the electro- and thermooptical behavior was studied of SLC layers that were uniformly oriented with their smectic layers along the electrodes by using surface-active materials, and it was shown possible to use such layers in practice in information-display devices.

b) The "guest-host" effect in mixed NLC. The ability of a NLC to orient the molecules of additives has been known for a long time, and it is currently used widely in spectroscopy.[124] The "guest-host" effect is observed when an electric field acts on a NLC (the host) containing as the additive (the guest) dye molecules that absorb light anisotropically (are pleochroic). If the additive molecule has an extended shape, it becomes oriented with its long axis along the molecules (the director) of the NLC. A time-average preferential orientation exists, since rotational movement of the additive molecules in the liquid crystal persists (just like the rotation of the molecules of the NLC itself). Owing to the orientation of the dye molecules, the liquid-crystalline solution shows dichroism of the optical absorption in the visible. The latter can be either positive ($D_{\parallel} > D_{\perp}$) or negative ($D_{\parallel} < D_{\perp}$),[125] depending on the orientation of the oscillator of the dipole transition **m** with respect to the long axis of the dissolved molecule ($D_{\parallel}$ and $D_{\perp}$ are the absorbances of the solution for light polarization vectors **e** parallel and perpendicular to the director of the NLC).

Figure 11a shows an ordinary electrooptical cell with an S-orientation of a NLC that has a positive dielectric anisotropy. A dye whose molecules have an extended shape is dissolved in the liquid crystal, and the absorption oscillator is parallel to the long axis of the molecule (this case is typical of dyes). In the absence of a field, the absorbance of the cell differs for light polarizations $e \parallel L$ ($D_{\parallel}$) and $e \perp L$ ($D_{\perp}$). When an electric potential that exceeds the threshold of the S-effect is applied to the cell (see Sec. a of Chap. 3), the liquid monocrystal becomes reoriented with its director along the field, and carries with it the dye molecules (Fig. 11b). In a strong enough field, the absorbances for light of any polarization become identical: $D_{\parallel}(\mathcal{E}) = D_{\perp}(\mathcal{E}) = D_{\perp}(\mathcal{E} = 0)$. Thus, there is a change in the absorbance $\Delta D_{\parallel}(\mathcal{E}) = D_{\parallel}(0) - D_{\parallel}(\mathcal{E})$ for light polarized along the initial position of the director. This effect was first observed in[126] and studied in greater detail in[127], where the electrooptical characteristics of cells were studied as a function of the dye concentration and the voltage (in particular, the maximum value of $\Delta D_{\parallel}$ proved to be ~1.5). The time characteristics of the "guest-host" effect obey the same relationships (9) and (10) as in deformation of a NLC by an electric field. Light switching by cells containing an initial B-orientation of the director (see Fig. 4c) is described in[128], while in[129] they studied the

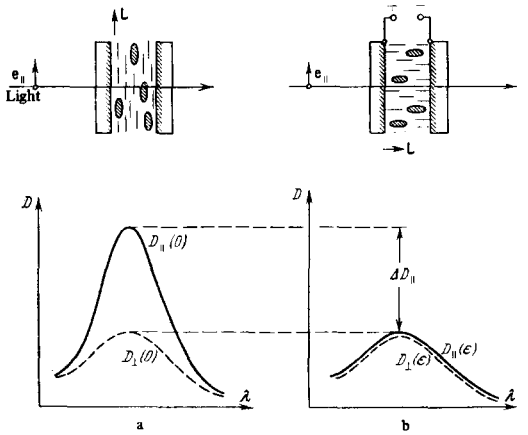

FIG. 11. The "guest-host" effect in NLC. a) Orientation of dye molecules and absorption spectra in polarized light in the absence of a field; b) the same, but with the field turned on. The dye molecules are cross-hatched.

anisotropy of luminescence of molecules dissolved in NLC.

c) The Kerr effect. At temperatures considerably above the temperature of phase transition to the isotropic liquid state (T_{NL}), substances that form liquid crystals behave in an electric field like ordinary (polar or nonpolar) liquids in showing the Kerr effect. However, as the temperature is lowered to approach T_{NL}, the Kerr constant of liquid-crystalline substances changes sign in some cases.[131] In other cases,[132,133] it increases sharply to attain values that exceed the Kerr constant of nitrobenzene by a factor of 200.[134] These anomalies are explained by the existence in the isotropic liquid of nuclei of the liquid-crystalline phase, i.e., molecular aggregates having short-range orientational order,[131,134] which greatly reduce the half-wave potential of the Kerr cell, and at the same time impair its speed of action to values of 10^{-7}—10^{-6} sec. In the nematic phase, the Kerr effect is completely masked by the other, stronger orientational effects discussed in Chap. 3.

6. CONCLUSION. POSSIBILITIES OF APPLYING VARIOUS ELECTROOPTICAL PHENOMENA

The principal feature of thin liquid-crystalline layers is their ability to change their optical properties when acted on by low voltages (several volts), with an extremely low power requirement (10^{-6}—10^{-4} W/cm^2). Hence, the different electrooptical effects based on the physical principles presented above are currently finding the most widespread practical application, or will do so in the next few years.[135] Intensive commercial development of compact devices is already being conducted (electronic wristwatches and calculators), with use of liquid-crystalline materials in their "dials," or indicators of numerical and alphabetic information.[5,136,137] Nematic crystals that show the T-effect or dynamic light scattering prove to be the most suitable for these devices, and also for analog scales of electrical measuring instruments.[138] The possibility is being studied intensively of making flat liquid-crystalline screens (like television screens) for displaying information on the real time scale by using dynamic scattering effects (and in particular, those showing "memory"), CLC → NLC phase transitions, etc.[137]

Owing to their improved speed of action, phase modulators of light that use the S-effect in NLC can be used in instruments for processing optical information, in holographic technique, in light deflectors, etc.[139] In combination with photosemiconductor films, liquid-crystalline layers can serve as amplifiers and image converters or as media for infrared photography.[140]

By using cholesteric and nematic liquid crystals, one can visualize an electric potential distribution in nondestructive testing of integral circuits and other objects.[141] The "guest-host" effect in doped NLC has been proposed for making color information indicators.[127,142] We can also assume that the anomalously large Kerr constants of ordered liquids[134] will make possible the design of rapid light modulators with lowered half-wave potentials.

[1)]There are also lyotropic liquid crystals that are formed in concentrated (generally aqueous) solutions of certain dyes, soaps, biological materials, etc. Their optical properties have hardly been studied, [80] and we shall discuss henceforth only therotropic liquid crystals.

[2)]This modulus characterizes the pure torsional deformation that would arise in the layers next to the wall in an electric field rotating about the axis Oz.

[3)]We are considering the bending B-deformation (see Fig. 7).

[4)]Apart from the numerical coefficient.

[5)]In [48,97] they did not take account of the boundary conditions at the electrodes of the cell, so that we must treat Eq. (25) and also (26) and (27) as being estimates.

[1] I. G. Chistyakov, Usp. Fiz. Nauk 89, 563 (1966) [Sov. Phys.-Uspekhi 9, 551 (1967)].
[2] I. G. Chistyakov, Zhidkie kristally (Liquid Crystals), "Nauka", M., 1970.
[3] G. W. Gray, Molecular Structure and Properties of Liquid Crystals, N.Y., Academic Press, 1962.
[4] G. H. Brown, J. W. Doane, and V. D. Neff, A Review of the Structure and Physical Properties of Liquid Crystals, L., Butterworths, 1971.
[5] J. Castellano, RCA Rev. 33, 296 (1972); A. Sussman, IEEE Trans. Parts, Hybrids and Packaging PHP-8, 24 (1972); L. Creagh, Proc. IEEE 61, 814 (1973).
[6] A. P. Kapustin, Elektroopticheskie i akusticheskie svoĭstva zhidkikh kristallov (Electrooptical and Acoustic Properties of Liquid Crystals), Nauka, M., 1973.
[7] W. Zwetkoff, Acta Physicochim. URSS 16, 132 (1942).
[8] I. Björnstahl, Ann. d. Phys. 56, 161 (1918).
[9] G. Friedel, Ann. de Phys. 19, 273 (1922); H. Zocher and V. Birstein, Zs. Phys. Chem. A142, 186 (1929), M. Jezewski, Zs. Phys. 51, 159 (1928); W. Kast, Zs. Kristallogr. 79, 146 (1931).
[10] V. K. Freedericksz and V. N. Tsvetkov, Dokl. Akad. Nauk SSSR 9, No. 4, 123 (1935); Acta Physicochim. URSS 3, 880 (1935).
[11] V. N. Tsvetkov, Uch. zap. Leningr. ped. in-ta 10, 5 (1938).
[12] W. N. Zwetkoff, Acta physicochim. URSS 6, 885 (1937).
[13] F. C. Frank, Disc. Farad. Soc. 25, 19 (1958).
[14] H. Gruler, T. J. Scheffer, and G. Meier, Zs. Naturforsch. 27a, 966 (1972).
[15] P. D. Berezin, I. N. Kompanets, V. V. Nikitin, and S. A. Pikin, Zh. Eksp. Teor. Fiz. 64, 599 (1972) [Sov. Phys.-JETP 37, 305 (1973)].
[16] H. J. Deuling, Mol. Cryst. and Liquid Cryst. 19, 123 (1972).
[17] A. Saupe, Zs. Naturforsch. 15a, 815 (1960); P. Pincus, J. Appl. Phys. 41, 974 (1970).
[18] F. M. Leslie, Mol. Cryst. and Liquid Cryst. 12, 57 (1970).
[19] H. Gruler, Zs. Naturforsch. 28a, 474 (1973).
[20] E. Jakeman and E. P. Raynes, Phys. Lett. A39, 69 (1972); Orsay Liquid Crystal Group, J. Chem. Phys. 51, 816 (1969).
[21] F. J. Kahn, Appl. Phys. Lett. 22, 386 (1973); E. J. Kahn, G. N. Taylor, and H. Shonhorn, Proc. IEEE 61, 823 (1973).
[22] P. Chatelain, Bull. Soc. franc. miner 66, 105 (1943).
[23] D. Berreman, Phys. Rev. Lett. 28, 1683 (1972).
[24] J. L. Janning, Appl. Phys. Lett. 21, 173 (1972).
[25] J. E. Proust, L. Ter-Minassian-Saraga, and E. Guyon, Sol. State Comm. 11, 1227 (1972); I. Haller, J. Chem. Phys. 57, 1400 (1972); T. Uchida and H. Watanabe, Japan. J. Appl. Phys. 11, 1559 (1972).
[26] V. Neff, L. Gulrich, and G. Brown, Mol. Cryst. 1, 225 (1966).
[27] T. Ohtsuka and M. Tsukamoto, Japan. J. Appl. Phys. 10, 1046 (1973).
[28] N. G. Basov, P. D. Berezin, L. M. Blinov, I. N.

Kompanets, V. N. Morozov, and V. V. Nikitin, ZhÉTF Pis. Red. 15, 200 (1972) [JETP Lett. 15, 138 (1972)]; P. D. Berezin, L. M. Blinov, I. N. Kompanets, and V. V. Nikitin, in Kvantovaya élektronika, No. 1 (13), 127 (1973) [Sov. J. Quant. Electr. 3 (1973)].
[29] a) M. F. Schiekel and K. Fahrenschon, Appl. Phys. Lett. 19, 391 (1971); b) R. A. Soref and M. J. Rafuse, J. Appl. Phys. 43, 2029 (1971).
[30] H. Gruler and G. Meier, Mol. Cryst. and Liquid Cryst. 16, 299 (1972).
[31] M. Hareng, E. Leiba, and G. Assouline, ibid. 17, 361; Appl. Opt. 11, 2920 (1972).
[32] M. Schadt and W. Helfrich, Appl. Phys. Lett. 18, 127 (1971).
[33] M. Schadt, J. Chem. Phys. 56, 1494 (1972); C. J. Alder and E. P. Raynes, J. Phys. D6, L33 (1973).
[34] G. Elliot, D. Harvey and M. Williams, Electron. Lett. 9, 399 (1973).
[35] A. Boller, H. Scheffer, M. Schadt, and P. Wild, Proc. IEEE 60, 1002 (1972); G. W. Gray, K. J. Harrison, and J. A. Nash, Electron. Lett. 9, 130 (1973); A. Ashford, J. Constant, J. Kirton, and E. P. Raynes, ibid., p. 118.
[36] A. Saupe, Angew. Chem. J. 80, 99 (1968); N. D. Samodurova and A. S. Sonin, Uch. zap. Ivanovsk ped. in-ta 99, 89 (1972).
[37] R. Meyer, Phys. Rev. Lett. 22, 918 (1969); R. Meyer and P. Pershan, Sol. State Comm. 13, 989 (1973).
[38] W. Haas, J. Adams, and J. Flannery, Phys. Rev. Lett. 25, 1326 (1970).
[39] D. Schmidt, M. Schadt, and W. Helfrich, Zs. Naturforsch 27a, 277 (1972).
[40] W. Helfrich, ibid. 26a, 833 (1971).
[41] A. P. Kapustin and L. K. Vistin', Kristallografiya 10, 118 (1965) [Sov. Phys.-Cryst. 10, 95 (1965)].
[42] R. Williams and G. Heilmeier, J. Chem. Phys. 44, 638 (1966).
[43] H. Gruler and G. Meier, Mol. Cryst. and Liquid Cryst. 12, 289 (1971).
[44] G. I. Sprokel, ibid. 22, 249 (1973).
[45] A. R. Von Hippel, Dielectrics and Waves, MIT Press, Sec. 31.
[46] a) D. McLemore and E. F. Carr, J. Chem. Phys. 57, 3245 (1972); F. Rondelez, Sol. State Comm. 11, 1675 (1972); b) W. Flint and E. F. Carr, Mol. Cryst. and Liquid Cryst. 22, 1 (1973).
[47] V. N. Tsvetkov and G. M. Mikhaĭlov, Acta Physicochim. URSS 8, 77 (1938); E. F. Carr, J. Chem. Phys. 39, 1979 (1963).
[48] W. Helfrich, ibid. 51, 4092 (1969).
[49] R. Williams, J. Chem. Phys. 39, 384 (1963); A. P. Kapustin and L. S. Larionova, Kristallografiya 9, 297 (1964) [Sov. Phys.-Cryst. 9, L. K. Vistin' and A. P. Kapustin, Kristallografiya 14, 741 (1969) [Sov. Phys.-Cryst. 14,
[50] S. A. Pikin, Zh. Eksp. Teor. Fiz. 60, 1185 (1971) [Sov. Phys.-JETP 33, 641 (1971)]; S. A. Pikin and A. A. Shtol'berg, Kristallografiya 18, 445 (1973) [Sov. Phys.-Cryst. 18, 283 (1973)].
[51] a) P. A. Penz and G. W. Ford, Phys. Rev. A6, 414, 1 1676 (1972); b) P. A. Penz, 4th Intern. Conference on Liquid Crystals, Kent, USA, 1972, Rept. No. 108.
[52] a) Orsay Liquid Crystal Group, Phys. Rev. Lett. 25, 1642 (1970); b) E. Dubois-Violette, P. G. de Gennes, and O. Parodi, J. de Phys. 32, 305 (1971).
[53] F. M. Leslie, Quart. J. Mech. and Appl. Math. 19, 357 (1966).
[54] L. K. Vistin', Dokl. Akad. Nauk SSSR 194, 1318 (1970) [Sov. Phys.-Doklady 15, 908 (1971)], Kristallografiya 15, 594 (1970) [Sov. Phys.-Cryst. 15, 514 (1970)].
[55] W. Greubel and V. Wolff, Appl. Phys. Lett. 19, 213 (1971).
[56] S. A. Pikin, Zh. Éksp. Teor. Fiz. 61, 2133 (1971) [Sov. Phys.-JETP 34, 1137 (1972)].
[57] W. H. de Jeu and C. J. Gerritsma, J. Chem. Phys. 56, 4752 (1972); W. H. de Jeu, C. J. Gerritsma, P. Van Zanten, and W. J. A. Goossens, Phys. Lett. A39, 355 (1972).
[58] M. F. Grebenkin, G. S. Chilaya, V. T. Lazareva, K. V. Roĭtman, L. M. Blinov, and V. V. Titov, Collected papers of the 2nd All-Union Scientific Conference on Liquid Crystals (Ivanovo, June 27–29, 1972), IK AN SSSR–IGPI, Ivanovo, 1973, p. 179.
[59] W. H. de Jeu, C. J. Gerritsma, and A. M. Van Boxtel, Phys. Lett. 34, 203 (1971).
[60] P. A. Penz, Phys. Rev. Lett. 24, 1405 (1970).
[61] M. Bertolotti, S. Lagomarsino, F. Scudieri, and D. Sette, J. Phys. C6, L177 (1973).
[62] D. Meyerhofer and A. Sussman, Appl. Phys. Lett. 20, 337 (1972).
[63] a) Orsay Liquid Crystal Group, in "Liquid Crystals 3", Ed. G. Brown and M. Labes, pt. II, L.–N.Y.–P., Gordon and Breach Sci. Publ., 1973, p. 711; b) Y. Galerne, G. Durand, and M. Veyssie, Phys. Rev. A6, 484 (1972).
[64] G. H. Heilmeier and W. Helfrich, Appl. Phys. Lett. 16, 155 (1970).
[65] C. Deutch and P. Keating, J. Appl. Phys. 40, 4069 (1969); E. W. Aslaksen and B. Ineichen, ibid. 42, 882 (1971).
[66] T. O. Carrol, J. Appl. Phys. 43, 767 (1972).
[67] N. Felici, Rev. Gen. Electr. 78, 17 (1969); N. Felici and R. Tobazeon et al., Proc. IEEE 60, 241 (1972).
[68] R. Turnball, J. Phys. D6, 1745 (1973).
[69] H. Koelmans and A. M. Van Boxtel, Phys. Lett. A32, 32 (1970).
[70] A. Takase, S. Sakagami and M. Nakamizo, Japan J. Appl. Phys. 12, 1255 (1973).
[71] L. K. Vistin' and A. P. Kapustin, Optika i Spektroskopiya 24, 650 (1968)
[72] G. H. Heilmeier, L. A. Zanoni, and L. A. Barton, Proc. IEEE 56, 1162 (1968); IEEE Trans. Electron Dev. ED-17, 22 (1970).
[73] S. A. Pikin, Zh. Éksp. Teor. Fiz. 63, 1115 (1972) [Sov. Phys.-JETP 36, 588 (1972)].
[74] T. O. Carroll, J. Appl. Phys. 43, 1342 (1972).
[75] L. D. Landau and E. M. Lifshitz, Élektrodinamika sploshnykh sred (Electrodynamics of Continuous Media), Fizmatgiz, M., 1959, Chap. 14 (Engl. Transl., Pergamon Press, Oxford, 1960).
[76] D. Jones, L. Greagh and S. Lu, Appl. Phys. Lett. 16, 61 (1970); G. Assouline and E. Leiba, Rev. Techn. Thomson–CSF 1, 483 (1969).
[77] L. T. Creagh, A. R. Kmetz, and R. A. Reynolds, IEEE Trans. Electron. Dev. ED-18, 672 (1971); L. S. Cosentino, ibid., p. 1192; C. H. Cooch and H. A. Tarry, J. Phys. D5, 125 (1972); M. F. Grebenkin et al., Kristallografiya 18, 429 (1973) [Sov. Phys.-Cryst. 18, 274 (1973)].
[78] A. Sussman, Appl. Phys. Lett. 21, 269 (1972); J. Nehring and M. S. Petty, Phys. Lett. A40, 307 (1972); R. Chang, J. Appl. Phys. 44, 1885 (1973).
[79] A. I. Baise, I. Teucher, and M. Labes, Appl. Phys. Lett. 21, 142 (1972); F. E. Wargocki and A. Lord, J. Appl. Phys. 44, 531 (1973).
[80] P. A. Winsor, J. Colloid Sci. 10, 101 (1955); T. Tachi-

bana and M. Tanaka, Bull. Chem. Soc. Japan **44**, 116 (1971).
[81] I. G. Chistyakov and V. N. Aleksandrov, Uch. zap. Ivanovsk. ped. in-ta 77, 34 (1970).
[82] F. Rondelez, H. Arnould and C. J. Gerritsma, Phys. Rev. Lett. **28**, 735 (1972).
[83] C. Mauguin, Bull. Soc. franc. miner. **34**, 71 (1911).
[84] H. L. de Vries, Acta Cryst. **4**, 215 (1951).
[85] R. B. Meyer, Appl. Phys. Lett. **14**, 208 (1969).
[86] C. J. Gerritsma and P. van Zanten, Mol. Cryst. and Liquid Cryst. **15**, 257 (1971).
[87] W. Helfrich, J. Chem. Phys. **55**, 839 (1971).
[88] J. H. Muller, Zs. Naturofrsch. **20a**, 849 (1965); Mol. Cryst. **2**, 167 (1966); W. J. Harper, ibid., p. 325.
[89] P. G. de Gennes, Sol. State Comm. **6**, 163 (1968); R. Meyer, Appl. Phys. Lett. **12**, 281 (1968).
[90] J. J. Wysocki, J. Adams and W. Haas, Phys. Rev. Lett. **20**, 1024 (1968).
[91] H. Baessler and M. Labes, ibid. **21**, 1791; F. J. Kahn, ibid. **24**, 209 (1970).
[92] H. Baessler and M. Labes, J. Chem. Phys. **51**, 5397 (1969).
[93] a) G. H. Heilmeier and J. E. Goldmacher, J. Chem. Phys. **51**, 1258 (1969); b) G. H. Heilmeier, L. A. Zanoni, and J. E. Goldmacher, in Liquid Crystal and Ordered Fluids, Ed. J. Johnson and R. Porter, Plenum Press, N.Y., 1970, p. 215.
[94] T. Ohtsuka and M. Tsukamoto, Japan J. Appl. Phys. **12**, 22 (1973); R. A. Kashnow, J. E. Bigelow, H. E. Cole, and C. R. Stein, Appl. Phys. Lett. **23**, 290 (1973).
[95] C. J. Gerritsma and P. van Zanten, Phys. Lett. **A42**, 127 (1972).
[96] E. Sackmann, S. Meiboom, and L. Snyder, J. Am. Chem. Soc. 89, 5981 (1967); P. B. Meyer, Appl. Phys. Lett. **14**, 208 (1968); G. Durand, L. Leger, F. Rondelez, and M. Veyssie, Phys. Rev. Lett. **22**, 227 (1969).
[97] W. Helfrich, Appl. Phys. Lett. **17**, 531 (1970).
[98] C. J. Gerritsma and P. van Zanten, Phys. Lett. **A37**, 47 (1971).
[99] a) T. J. Scheffer, Phys. Rev. Lett. **28**, 593 (1972); b) F. Rondelez, H. Arnould, and C. J. Gerritsma, ibid., p. 735.
[100] J. P. Hurault, J. Chem. Phys. **59**, 2068 (1973).
[101] F. Rondelez and J. P. Hulin, Sol. State Comm. **10**, 1009 (1972).
[102] H. Baessler and M. Labes, J. Chem. Phys. **51**, 1846 (1969); H. Baessler, T. M. Laronge, and M. Labes, ibid., p. 3213.
[103] C. J. Gerritsma and P. van Zanten, Phys. Lett. **A42**, 329 (1972).
[104] N. Oron and M. Labes, Appl. Phys. Lett. **21**, 243 (1972).
[105] J. Wysocki, J. Adams and W. Haas, Mol. Cryst. and Liquid Cryst. **8**, 471 (1969).
[106] C. J. Gerritsma, ibid. **15**, 257 (1971).
[107] G. H. Heilmeier and J. E. Goldmacher, Appl. Phys. Lett. **13**, 132 (1969); Proc. IEEE **57**, 34 (1969).
[108] a) W. Haas, J. Adams, and J. B. Flannery, Phys. Rev. Lett. **24**, 577 (1970); b) W. Haas, J. Adams, and G. Dir, Chem. Phys. Lett. **14**, 95 (1972).
[109] G. S. Chilaya, V. T. Lazareva, and L. M. Blinov, Kristallografiya 18, 203 (1973) [Sov. Phys.-Cryst. **18**, 127 (1973)].
[110] F. Rondelez and A. Arnould, C. R. Ac. Sci. **B273**, 549 (1971).
[111] B. Kerlleñevich and A. Coche, J. Appl. Phys. **42**, 5313 (1971).
[112] L. Melamid and D. Rubin, Appl. Phys. Lett. **16**, 149 (1969); J. Wysocki, J. Adams, and W. Haas, Mol. Cryst. and Liquid Cryst. **8**, 471 (1969); W. Haas and J. Adams, J. Electrochem. Soc. **118**, 1372 (1969).
[113] J. P. Hulin, Appl. Phys. Lett. **21**, 455 (1972).
[114] W. Maier and G. Meier, Zs. Phys. Chem. **13**, 251 (1957).
[115] E. F. Carr, Phys. Rev. Lett. **24**, 807 (1970); references in [63a], p. 727.
[116] L. Chou and E. F. Carr, Phys. Rev. **A7**, 1639 (1973).
[117] I. G. Chistyakov, I. V. Sushkin, V. M. Chaĭkovskiĭ, and E. A. Kosterin, Uch. zap. Ivanovsk ped. in-ta 77, 3 (1970).
[118] R. Wise, D. Smith, and J. Doane, 4th Intern. Conference on Liquid Crystals, Kent, USA, 1972, Rept. No. 30.
[119] V. Freedericksz and A. Repjeva, Acta Physicochim. URSS **4**, 91 (1936).
[120] L. K. Vistin' and A. P. Kapustin, Kristallografiya **13**, 349 (1968) [Sov. Phys.-Cryst. **13**, 284 (1968)].
[121] R. A. Soref, "The Physics of Opto-Electronic Materials", Ed. W. A. Albers, Jr., N.Y.-L., Plenum Press, 1971, p. 207, C. Tani, Appl. Phys. Lett. **19**, 241 (1971).
[122] J. A. Geurst and W. J. A. Goossens, Phys. Lett. **A41**, 369 (1972).
[123] F. J. Kahn, Appl. Phys. Lett. **22**, 111 (1973).
[124] A. Saupe, Mol. Cryst. and Liquid Cryst. **16**, 87 (1972).
[125] E. Sackmann, J. Am. Chem. Soc. 90, 3569 (1968); L. Pohl, Kontakte (Merck), Nr. 1, 33 (1973).
[126] G. H. Heilmeier and L. A. Zanoni, Appl. Phys. Lett. **13**, 91 (1968).
[127] J. A. Castellano, Electronics **43**, 64 (1970).
[128] J. A. Castellano, reference in [93b], p. 293.
[129] E. Sackmann, Chem. Phys. Lett. **4**, 537 (1970); G. Bauer, A. Stieb and G. Meier, J. Appl. Phys. **44**, 1905 (1973).
[130] P. G. de Gennes, Comm. Sol. State Phys. **3**, 35 (1968).
[131] V. N. Tsvetkov and E. I. Ryumtsev, Kristallografiya **13**, 290 (1968) [Sov. Phys.-Cryst. **13**, 225 (1968)].
[132] J. C. Filippini, C. R. Ac. Sci. **B275**, 349 (1972).
[133] A. R. Johnston, J. Appl. Phys. **44**, 2971 (1973).
[134] M. Schadt and W. Helfrich, Mol. Cryst. and Liquid Cryst. **17**, 355 (1972).
[135] Liquid Crystals and Their Applications, Ed. T. Kallard, N.Y., Optosonic Press, 1970.
[136] G. H. Heilmeier, Sci. Amer. **222** (4), 100 (1970), N. A. Luce, Electronics **45**, 93 (1972).
[137] L. A. Goodman, J. Vac. Sci. and Technol. **10**, 804 (1973).
[138] R. A. Soref, Appl. Opt. **9**, 1323 (1970); Proc. IEEE **61**, 384 (1973).
[139] I. N. Kompanets, P. D. Berezin, A. A. Vasil'ev, V. V. Nikitin, and L. M. Blinov, reference in [58], p. 274.
[140] J. D. Margerum, J. Nimoy and S. Y. Wong, Appl. Phys. Lett. **17**, 51 (1970); G. Assouline, M. Hareng, and E. Leiba, Proc. IEEE **59**, 1355 (1971); M. I. Barnik and L. M. Blinov, Abstracts of the 1st All-Union Conference on Non-Silver and Unusual Photographic Processes, Part 2, Kiev State University, Kiev, 1972, p. 45.
[141] K. Thiessen and T. Le Tuyen, Phys. Stat. Sol. **a13**, 73 (1972).
[142] E. Gordon and L. Anderson, Proc. IEEE, **61**, 807 (1973).
[143] S. G. Dmitriev, Zh. Éksp. Teor. Fiz. **61**, 2049 (1971) [Sov. Phys.-JETP **34**, 1093 (1972)].
[144] M. F. Grebënkin, M. I. Barnik, L. M. Blinov, and V. V. Titov, Abstracts of the 1st All-Union Scientific-Technical Conference "Photometric Measurements and Their Metrological Realization," M., 1974, p. 86.
[145] I. G. Chistyakov and L. K. Vistin', Kristallografiya **19**, 195 (1974) [Sov. Phys.-Cryst. **19**, 119 (1974)].
[146] G. Labrunie and J. Robert, J. Appl. Phys. **44**, 4869 (1973).
[147] H. Hervet, J. P. Hurault and F. Rondelez, Phys. Rev. **A8**, 3055 (1973).

Translated by M. V. King